REPÚBLICA FEDERATIVA DO BRASIL
MINISTÉRIO DA EDUCAÇÃO

UFCSPA
UNIVERSIDADE FEDERAL DE CIÊNCIAS DA SAÚDE DE PORTO ALEGRE
PROGRAMA DE PÓS-GRADUAÇÃO EM CIÊNCIAS DA SAÚDE

Thiago Casarin Hartmann

CÓRTEX CINGULADO E SUAS SUBDIVISÕES: PROTOCOLO DE SEGMENTAÇÃO MANUAL EM RESSONÂNCIA MAGNÉTICA

Porto Alegre
2014

Thiago Casarin Hartmann

CÓRTEX CINGULADO E SUAS SUBDIVISÕES: PROTOCOLO DE SEGMENTAÇÃO MANUAL EM RESSONÂNCIA MAGNÉTICA

Dissertação de Mestrado apresentada ao Programa de Pós-Graduação em Ciências da Saúde da Universidade Federal de Ciências da Saúde de Porto Alegre, como requisito parcial para a obtenção do título de Mestre em Ciências da Saúde.

Orientador: Prof. Dr. Ygor Arzeno Ferrão

Co-orientador: Prof. Dr. Pedro Rosa-Neto

Porto Alegre
2014

Catalogação na Publicação

Hartmann, Thiago Casarin
Córtex Cingulado e suas subdivisões : protocolo de segmentação manual em ressonância magnética / Thiago Casarin Hartmann. -- 2014.
93 f. : il., tab. ; 30 cm.

Dissertação (mestrado) -- Universidade Federal de Ciências da Saúde de Porto Alegre, Programa de Pós-Graduação em Ciências da Saúde, 2014.

Orientador(a): Prof. Dr. Ygor Arzeno Ferrão ; coorientador(a): Prof. Dr. Pedro Rosa-Neto.

1. Neuroimagem. 2. Giro do Cíngulo. 3. Neuroanatomia. 4. Protocolos. 5. Espectroscopia de Ressonância Magnética. I. Título.

Sistema de Geração de Ficha Catalográfica da UFCSPA com os dados fornecidos pelo(a) autor(a).

REPÚBLICA FEDERATIVA DO BRASIL
MINISTÉRIO DA EDUCAÇÃO

UFCSPA

UNIVERSIDADE FEDERAL DE CIÊNCIAS DA SAÚDE DE PORTO ALEGRE

CERTIFICADO

Certificamos, para os devidos fins, que **Thiago Casarin Hartmann**, apresentou a dissertação de mestrado no dia 1º de outubro de 2014, intitulada "Córtex Cingulado e suas Subdivisões: Protocolo de Segmentação Manual em Ressonância Magnética", orientada pelo professor Ygor Arzeno Ferrão, desenvolvida no Programa de Pós-Graduação em Ciências da Saúde da UFCSPA, tendo sido considerado aprovado.

Porto Alegre, 1º de outubro de 2014.

CRISTIANE MONDADORI
Secretária Executiva
Pós-Graduação - UFCSPA

AGRADECIMENTOS

- Ao professor Ygor, pela inspiração e apoio constantes.
- Ao professor Pedro, pela paciência e pelo conhecimento.
- Aos acadêmicos Paola, Daniel e João, pelo inestimável esforço e compreensão.
- À minha mãe, Maria das Graças Casarin Hartmann; meu pai, Celso Antônio Hartmann (*in memoriam*), e minha irmã Angélica Casarin Hartmann, sempre presentes na minha vida.
- A todo o grupo de pesquisa do Centro de Estudos em Envelhecimento da McGill.
- A todos os envolvidos direta ou indiretamente com o presente trabalho.
- Em especial, à minha amada Raquel, sem ela nada teria sabor.

SUMÁRIO

1. LISTA DE FIGURAS DA INTRODUÇÃO

2. RESUMO

O CÓRTEX CINGULADO E SUAS SUBDIVISÕES: PROTOCOLO DE SEGMENTAÇÃO MANUAL EM RESSONÂNCIA MAGNÉTICA

Introdução: O giro do cíngulo forma o componente dorsal do lobo límbico de Broca e tem um papel central na maioria das teorias das emoções. Uma das técnicas mais utilizadas para estudos em neuroimagem é a análise de regiões de interesse através de parcelamento manual em ressonância magnética. Existem vários protocolos de parcelamento manual para regiões do giro do cíngulo, mas não há um consenso sobre o melhor modo de fazê-la. Neste trabalho, são analisados os protocolos existentes e é proposta uma unificação do método, além de uma tentativa de definições de subdivisões mais baseada em critérios histológicos até então não considerados (por exemplo, o campo gigantopiramidal de Braak).

Métodos: Foi desenvolvido um protocolo de parcelamento de todo o córtex cingulado, aplicado por três avaliadores para testar sua replicabilidade num total de 8 imagens de ressonância magnética do cérebro de pacientes com déficit cognitivo leve e controles. O programa usado foi o Display para Linux, que possibilita o parcelamento das regiões de interesse com visualização interativa simultânea de todos os eixos. Foi proposta uma divisão em 7 regiões do córtex cingulado para cada hemisfério e um novo marcador estereotáxico para delimitação entre as regiões posterior e anterior.

Resultados: Os coeficientes de correlação intraclasse foram satisfatórios para a maioria das regiões. Os resultados foram melhores para as regiões maiores, as menores necessitam revisão. Mapas probabilísticos foram gerados para avaliar as regiões de maior concordância.

Conclusão: Um novo método de parcelamento do córtex cingulado foi desenvolvido, com recomendações para o uso de novos marcadores para separação de suas regiões.

Palavras-chave: córtex cingulado, parcelamento, ressonância magnética, volumetria, giro do cíngulo

3. ABSTRACT

THE CINGULATE CORTEX AND ITS SUBDIVISIONS: MANUAL PARCELLATION PROTOCOL IN MAGNETIC RESONANCE IMAGING

Introduction: The cingulate gyrus forms the dorsal component of Broca's limbic lobe and has a central role in most theories of emotions. One of the most used techniques in neuroimaging studies is the analysis of regions of interest by manual parcellation on magnetic resonance images. There are many manual parcellation protocols for regions of the cingulate gyrus, but there is no consensus of the best way to do it. In this study, existing protocols are analyzed to propose a unified method and an attempt of new subdivisions, based more on histological criteria hitherto not considered (for example, the Braak's gigantopiramidal field).

Methods: A whole cingulate cortex parcellation protocol was developed and applied by three raters to test its replicability in 8 magnetic resonance images from brains of mild cognitive impairment patients and controls. The software used was Display for Linux, which permits the parcellation of regions of interest with simultaneous interactive visualization of all axes. A cingulate cortex 7 regions division for each hemisphere was proposed and a new stereotaxic landmark was delineated for the border between the anterior and posterior cingulate cortices.

Results: The intraclass correlation coefficients were satisfactory for most regions. Results were better for larger regions, smaller regions need revision. Probabilistic maps were generated to evaluate concordant regions.

Conclusion: A new method of cingulate cortex parcellation was developed, with recommendations for the use of new landmarks to separate its regions.

Keywords: cingulate cortex, parcellation, MRI, volumetrics, cingulate gyrus.

4. ABREVIATURAS

acals: *anterior calcarine sulcus* (sulco calcarino anterior)

ACC: *anterior cingulate cortex* (córtex cingulado anterior)

ascs: *anterior subcallosal sulcus* (sulco subcaloso anterior)

cas: *callosal sulcus* (sulco caloso)

cc: *corpus callosum* (corpo caloso)

CCA: córtex cingulado anterior

CCP: córtex cingulado posterior

cgs: *cingulate sulcus* (sulco cingulado)

CMR: *caudomedial region* (região caudomedial)

CSF: *cerebrospinal fluid* (fluido cerebroespinhal)

dACC: *dorsal anterior cingulate cortex* (córtex cingulado anterior dorsal)

DBS: *deep brain stimulation* (estimulação cerebral profunda)

GM: *gray matter* (matéria cinzenta)

ICC: *intraclass correlation coefficient* (coeficiente de correlação intraclasse)

IRM: imagem de ressonância magnética

MCSA: *McGill Center for Studies in Aging* (Centro de Estudos em Envelhecimento da McGill)

MNI: *Montreal Neurological Institute* (Instituto Neurológico de Montreal)

mr: *marginal ramus* (ramo marginal)

MRI: *magnetic resonance image* (imagem de ressonância magnética)

PCC: *posterior cingulate cortex* (córtex cingulado posterior)

pscs: *posterior subcallosal sulcus* (sulco subcaloso posterior)

rACC: *rostral anterior cingulate cortex* (córtex cingulado anterior rostral)

RF: radiofrequência

ROI: *region-of-interest* (região de interesse)

RSC: *retrosplenial cortex* (córtex retroesplenial)

sACC: *subcallosal anterior cingulate cortex* (córtex cingulado anterior subcaloso)

SGC: *subgenual cortex* (córtex subgenual)

spls: *splenial sulcus* (sulco esplenial)

srs: *superior rostral sulcus* (sulco superior rostral)

TC: tomografia computadorizada

TCC: terapia cognitivo-comportamental

TOC: transtorno obsessivo-compulsivo

VBM: *voxel-based morphometry*

WM: *white matter* (matéria branca)

5. INTRODUÇÃO

Desde as descobertas pioneiras de Santiago Ramón Y Cajal no final do século XIX e início do século XX, que o levaram à criação da "doutrina do neurônio" (*neuron doctrine*), tem havido um interesse crescente na busca por uma interface entre a mente e o cérebro. Esse interesse e as descobertas de Ramón Y Cajal lançaram as bases para a fundação da moderna neurociência (Kandel & Squire, 2000). Antes, e até meados da década de 70, a psiquiatria e a psicologia estavam enraizadas no dualismo cartesiano, ou seja, havia uma dicotomia entre o cerebral e o mental, admitindo-se que o cérebro era necessário para a plenitude do desenvolvimento mental, apenas isso (Hyman, 2005). Segundo o dualismo cartesiano, a substância da mente seria diferente da substância do cérebro (Kandel *et al.,* 2000). Até mesmo Freud tentou abolir o dualismo com seu Projeto Para uma Psicologia Científica (1895), publicado postumamente em 1950, pois seu autor tentou destruí-lo, já que desistira de unir a mente e o cérebro ao longo de seu trabalho, focando-o somente na primeira.

O advento da neuroimagem, sobretudo a funcional, contribuiu substancialmente para a derrocada do dualismo em favor do desenvolvimento da neurociência, possibilitando o estudo de processos psicológicos e cognitivos *in vivo* no ser humano (Kandel & Squire, 2000). A imagem de estruturas internas do ser humano data do século XIX, com a descoberta dos raios-X, realizada por Roentgen. Entretanto, foi só em 1971, com a produção da primeira tomografia computadorizada (TC), que a neuroimagem moderna teve suas bases lançadas (Filler, 2009).

Ainda em 1971, o potencial da ressonância magnética vinha sendo explorado na medicina por Damadian, que identificou diferenças no tempo de relaxamento magnético em T_1 e T_2 entre células tumorais e normais de ratos. No entanto, ainda não se pensava em produção de imagens usando esta técnica. Somente em 1973, quando Paul Lauterbur publicou um pequeno artigo na Nature relatando como conseguira produzir imagens de pequenas quantidades de água usando ressonância magnética é que essa preocupação veio à tona. Interessantemente, seu artigo foi inicialmente rejeitado, pois os revisores acreditavam que a técnica seria de interesse limitado somente para especialistas (Filler, 2009).

Duas publicações clássicas ainda seriam necessárias para a disseminação do uso da imagem de ressonância magnética (IRM) tanto na pesquisa quanto na clínica médica. Em 1978, citando os trabalhos seminais de Lauterbur (1973) e Damadian (1971), Ernst publicou uma patente nos Estados Unidos de uma máquina que seria capaz de gerar imagens tridimensionais de objetos usando a ressonância magnética. Dois anos depois, em 1980,

Edelstein *et al.* publicaram o relato do invento de uma máquina que seria capaz de captar imagens de todo o corpo humano através da ressonância magnética. Seria possível, a partir de então, obter imagens do corpo humano, incluindo o cérebro, sem a necessidade de expor o paciente a doses altas de radiação como na TC ou no raio-X, e com uma resolução mais satisfatória.

5.1. PRINCÍPIOS BÁSICOS DA GERAÇÃO DE IMAGEM POR RESSONÂNCIA MAGNÉTICA

Para um melhor entendimento da aquisição de imagens através da ressonância magnética é necessário um estudo da mecânica quântica de partículas. A presente explanação é baseada nos trabalhos de Pykett et al. (1982), Hendee & Morgan (1984) e Scherzinger & Hendee (1985). A proliferação de revisões sobre os mecanismos físicos da técnica de ressonância magnética no início da década de oitenta pode ser entendida como reflexo do interesse e da curiosidade cada vez maior do meio acadêmico sobre ela.

Todas as partículas nucleares, isto é, prótons e nêutrons, têm um movimento intrínseco chamado spin. A maioria dos núcleos atômicos, no entanto, tem o mesmo número de prótons e nêutrons, o que faz com que o movimento spin de ambos se anule mutuamente. Isso não ocorre com o átomo de hidrogênio, cujo núcleo é constituído de somente um próton. Nesse caso, pelo fato de o núcleo conter uma carga elétrica, o movimento spin cria um pequeno campo magnético. Cada próton tem seu pequeno campo magnético orientado aleatoriamente (Figura 1). Quando um campo magnético externo é aplicado à amostra, os campos magnéticos dos prótons orientam-se no mesmo sentido do campo externo (Figura 2). Esse é o primeiro passo para a geração de imagem na máquina de ressonância magnética.

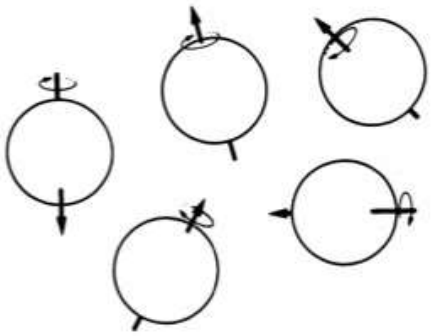

Figura 1: representação esquemática dos campos magnéticos de cada próton orientados aleatoriamente. As esferas representam os prótons, o vetor maior o sentido do campo magnético de cada um e o vetor menor o sentido do movimento giratório, isto é, o *spin*

(obtido de Pykett *et al.*, 1982).

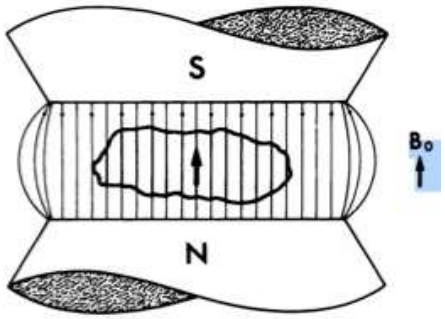

Figura 2: campo magnético aplicado à amostra (B_0) orienta o campo de todos os seus prótons para o mesmo sentido, no caso mostrado, norte → sul (obtido de Pykett *et al.*, 1982).

Após a etapa de reorientação dos campos magnéticos de cada próton, é aplicado um pulso de radiofrequência (RF) no sentido perpendicular ao do campo magnético externo (Figura 3). Os campos dos prótons sofrem uma deformação na direção do pulso aplicado, análoga à deformação de um pião perdendo sua força giratória (Figura 4). A este movimento, dá-se o nome de precessão. A precessão faz com que os prótons emitam um sinal de rádio, que pode ser captado por um receptor. A diferença na concentração de prótons entre os tecidos biológicos faz com haja uma diferença na quantidade de sinal de rádio que cada tecido emite no movimento de precessão. Tal diferença está intimamente relacionada com a quantidade de água presente nos tecidos biológicos, visto que a água tem alta concentração de prótons (H_2O), e, em menor grau, com a quantidade de lipídios. Logo, quanto mais água, maior o sinal detectado, tornando possível, numa imagem, a diferenciação dos tecidos biológicos com base no seu conteúdo aquoso.

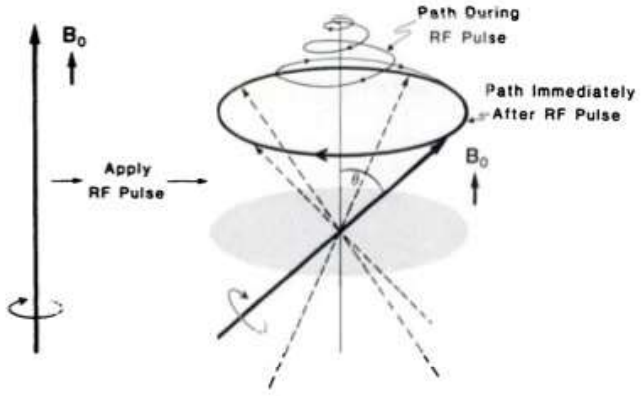

Figura 3: aplicação de um pulso de RF no campo magnético B_0 gera o movimento de precessão, representado à direita (obtido de Pykett *et al.*, 1982).

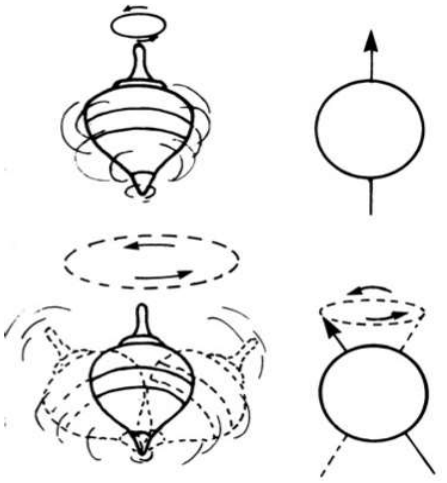

Figura 4: analogia entre o movimento de um pião, à esquerda, com o movimento de precessão, à direita (obtido de Hendee & Morgan, 1984).

Após a cessação do pulso de RF, a tendência do campo dos prótons é retornar ao estado anterior ao estímulo, ou seja, o mesmo sentido do campo magnético externo. Ao realizar este movimento de retorno, o qual denominamos T_1 ou relaxamento *spin*-rede, o sinal de rádio emitido pelos prótons vai gradativamente caindo. Esta diferença no sinal de rádio emitido também é passível de aferição, e ela é mais contrastante entre os diferentes tecidos biológicos que a simples densidade de prótons (v. parágrafo anterior), gerando imagens melhor definidas. Assim como a densidade de prótons, o T_1 também está relacionado com uma maior solidez ou aquosidade do tecido biológico: tecidos com maior solidez tendem a ter T_1 mais longos porque apresentam ligações químicas mais fortes entre os átomos.

O movimento de precessão não é homogêneo; existem várias oscilações, de sentido perpendicular ao do campo magnético externo, que acontecem principalmente após a cessação do pulso de RF aplicado e terminam após determinado tempo. Em outras palavras: o movimento de precessão demora um pouco para atingir o equilíbrio e formar um "cone" melhor desenhado (ver analogia com pião). Essa diminuição da heterogeneidade do movimento de precessão também gera mudanças no sinal emitido pelos prótons, e dá-se o nome de T_2, ou relaxamento *spin*-*spin*, para tal fenômeno (Figura 5). Também há diferenças no T_2 de cada tecido biológico, e, da mesma forma que o T_1, isso é explorado visando-se uma melhor visualização de estruturas na IRM.

O processo de formação de imagem ocorre de forma análoga à de uma TC. Detectores no aparelho conseguem captar a frequência do sinal de rádio emitido na precessão, em T_1 e T_2, conforme o intervalo de tempo em que se aplica os pulsos de RF perpendiculares ao campo

magnético externo. Cada faixa de frequência do sinal emitido pelos prótons é então traduzida computacionalmente para uma escala de tonalidade cinza para cada unidade de volume num plano cartesiano tridimensional e então temos a imagem (Figura 6). As unidades de volume na imagem recebem o nome de *voxel*, e correspondem a 1-2 mm^3 de tecido, dependendo principalmente da resolução do aparelho.

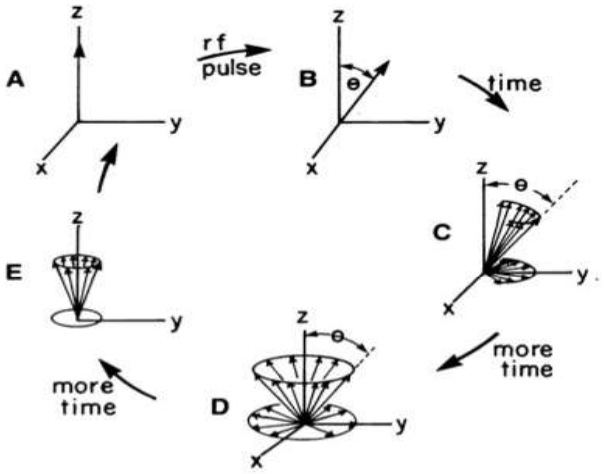

Figura 5: representação esquemática do relaxamento *spin-spin*. O momento A representa o próton com seu campo magnético orientado para o eixo z. Após a aplicação de um pulso de RF, no momento B, o vetor do campo se afasta do eixo z em direção aos eixos x e y. Segue-se no momento C o movimento de precessão de forma heterogênea, ainda um pouco desordenado. No momento D, o movimento de precessão encontra-se mais simétrico. É esse período entre C e D que recebe o nome de T_2, ou relaxamento *spin-spin* (obtido de Hendee & Morgan, 1984).

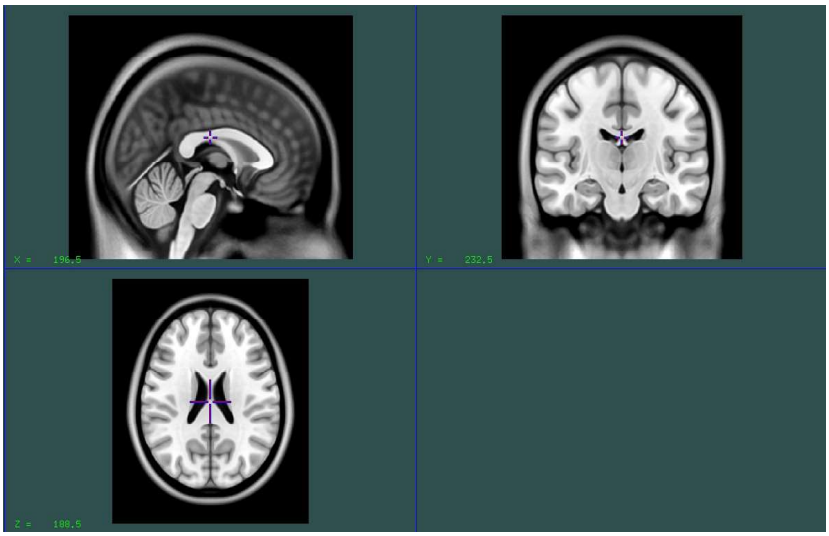

Figura 6: exemplo de imagem gerada em um plano cartesiano tridimensional. No canto inferior esquerdo de cada janela estão as coordenadas X, Y e Z da posição do cursor. Imagens

do atlas de Fonov *et al*. (2009).

Posteriormente, outras técnicas utilizando a IRM foram desenvolvidas, como a ressonância magnética funcional e a tractografia por tensor de difusão. Ambas são igualmente fascinantes, pois permitem estudar a ativação de determinadas áreas corticais sob a realização de tarefas e os caminhos axonais percorridos pelos neurônios, respectivamente. Entretanto, elas fogem ao escopo do presente trabalho, que é o estudo estrutural (morfométrico) do córtex cingulado. Para tal, bastam IRMs comuns.

5.2. TÉCNICAS UTILIZADAS PARA O ESTUDO DA MORFOMETRIA DE ESTRUTURAS ANATÔMICAS DO SISTEMA NERVOSO CENTRAL

Atualmente, a neuroimagem é capaz de revelar uma quantidade extraordinária de informações sobre as características estruturais, funcionais e bioquímicas do cérebro humano, sendo inclusive cogitada como desfecho para ensaios clínicos. De fato, já existem trabalhos correlacionando achados de neuroimagem com a resposta terapêutica. Hoexter *et al.* (2012), por exemplo, avaliaram alterações morfométricas na matéria cinzenta em pacientes com Transtorno Obsessivo-Compulsivo (TOC) em relação a pessoas saudáveis, antes e após tratamento com fluoxetina ou Terapia Cognitivo-Comportamental (TCC). Eles encontraram diferenças principalmente no putâmen esquerdo dos pacientes com TOC tratados com fluoxetina, mas não no grupo da TCC, apesar da resposta clínica sem diferença estatisticamente significativa entre os dois grupos. Valenzuela *et al*. (2011) fazem uma reflexão interessante sobre a utilização de parâmetros de neuroimagem como resposta anterior à resposta clínica de determinados tratamentos neuropsiquiátricos, sugerindo que o uso disseminado da neuroimagem como parte do desfecho de ensaios clínicos está próximo. Entretanto, os autores fazem a ressalva de que ainda precisamos de correlações mais claras entre a neuroimagem e a clínica.

Existem dois grandes grupos de técnicas utilizadas para o estudo estrutural do sistema nervoso central: as que utilizam a demarcação (ou segmentação, parcelamento) de regiões de interesse (*region-of-interest* – ROI) e as de cérebro inteiro (*whole brain techniques*). Entretanto, a maioria das técnicas, independentemente do grupo, requer um preparo das imagens antes de sua aplicação que chamamos de normalização espacial. Essa técnica consiste no uso de transformações matemáticas para colocar todos os cérebros da amostra no mesmo espaço estereotáxico padrão, corrigindo assim diferenças no tamanho total do cérebro

e na posição da cabeça durante o exame (Ashburner & Friston, 2004). Entende-se espaço estereotáxico padrão como um mesmo sistema de coordenadas cartesianas tridimensionais, sendo o mais utilizado o de Tailarach & Tournoux (1988), que propõe a comissura anterior como o ponto 0 dos três eixos do gráfico. Existem outros sistemas, como o do *Montreal Neurological Institute* (MNI) (Brett *et al*., 2001) e o de Sydney (Li *et al*., 2003).

Dentre as de cérebro inteiro, merece destaque a *voxel-based morphometry* (VBM), uma técnica automatizada de comparação *voxel* por *voxel*. A VBM foi descrita pela primeira vez por Ashburner & Friston (2000) e otimizada por Good *et al*. (2001). Essencialmente, consiste na sobreposição de diversas imagens cerebrais para verificação estatística das diferenças entre regiões. Divide-se em várias etapas: primeiro procede-se à normalização espacial das imagens; depois utiliza-se uma técnica de segmentação automática de matéria cinzenta, matéria branca e líquido cerebroespinhal; a próxima fase é a de modulação, onde se aplica um método Jacobiano para correção das deformações de volume provocadas pela normalização; após, usa-se a suavização para uma distribuição mais paramétrica dos dados, e então procede-se ao cálculo das diferenças estatisticamente significativas de intensidade dos *voxels*. As regiões com maior diferença de volume terão maior diferença entre a intensidade dos *voxels* sobrepostos. Percebe-se que mesmo com o uso de uma técnica de cérebro inteiro, é necessário um conhecimento das demarcações anatômicas das ROIs, para saber a qual estrutura pertencem os *voxels* que mostraram-se diferentes.

As técnicas de demarcação de ROIs podem ser manuais, semiautomáticas ou automáticas. As manuais consistem na descrição de marcadores anatômicos que delimitam a área a ser segmentada. Normalmente são formatadas como protocolos onde estão descritas regras bem detalhadas de como marcar as ROIs numa imagem. Como exemplo podemos citar os protocolos de Bonilha *et al.* (2004) e Entis *et al*. (2012); o primeiro trata da segmentação manual de estruturas temporais e o segundo propõe-se à segmentação manual da amígdala e suas subdivisões.

A maioria dos protocolos de demarcação de ROIs, no entanto, utiliza alguma técnica de segmentação automática prévia de matéria cinzenta, matéria branca e líquor. Existem vários algoritmos na literatura que podem ser usados para essa finalidade (Oguz, 2014; Harris, 1999). Quando utilizam alguma técnica automática concomitante à manual, diz-se que a demarcação da ROI é semiautomática. Como exemplos temos os protocolos de segmentação do córtex frontal de Ranta *et al*. (2009) e Crespo-Facorro *et al*. (1999), bem como os de algumas áreas do córtex cingulado (Fornito *et al*., 2006; Jones *et al*., 2006; McCormick *et al*., 2006).

Existem também as técnicas de demarcação de ROI completamente automatizadas. Como exemplo podemos citar a técnica desenvolvida e aperfeiçoada por Dale *et al*. (1999) e Fischl *et al*. (1999; 2002), que utiliza atlas probabilísticos das estruturas cerebrais. Tais atlas são confeccionados dando-se uma coordenada cartesiana tridimensional para determinado *voxel* e verificando-se qual a probabilidade de ele pertencer a determinada estrutura anatômica. Um dos *softwares* utilizados nessa técnica é o *Freesurfer*, desenvolvido na *Harvard University* (Fischl *et al*., 2004; Desikan *et al*., 2006; Salat *et al*. 2009).

A principal limitação das técnicas de segmentação manual de ROI (ou semiautomáticas, com separação de matéria cinzenta, branca e líquor) é o tempo necessário para sua execução. Além disso, elas requerem um observador com relativo treino para sua realização precisa, e por esse motivo, várias tentativas de sua substituição têm sido realizadas. No entanto, elas ainda são consideradas o padrão-ouro para o estudo de macrorregiões e/ou regiões de difícil separação entre substância branca e cinzenta, como o hipocampo (Geuze *et al*., 2005; Bergouignan *et al*., 2009; Hayes *et al*., 2014).

5.3. O CÓRTEX CINGULADO E SUA IMPORTÂNCIA PARA A NEUROPSIQUIATRIA

O giro do cíngulo é a estrutura cortical mais proeminente na face medial do cérebro humano. Ele forma um cinturão que se estende da lamina terminalis, rostral à comissura anterior, circundando o corpo caloso e terminando um pouco ventral ao esplênio do corpo caloso (Figura 7). O giro do cíngulo forma o componente dorsal do lobo límbico de Broca (1878 apud Vogt *et al*., 2004) e tem um papel central na maioria das teorias das emoções. A subdivisão mais clássica da sua região cortical engloba o córtex cingulado anterior, o posterior e o retroesplenial. (Vogt *et al*., 2004).

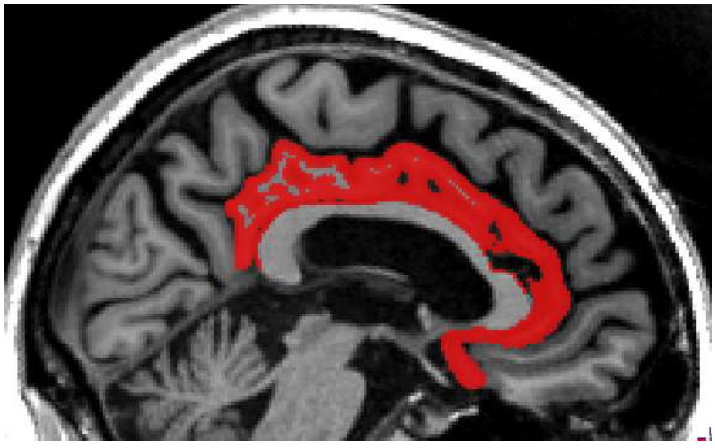

Figura 7: demarcação de todo o córtex cingulado, incluindo a área subgenual, em vermelho. Imagem da amostra.

O córtex cingulado é visto como integrador de processos emocionais e cognitivos (Shackman *et al*., 2011, Paus T., 2001). Papez (1937 apud Shackman *et al*., 2011), em um trabalho seminal, descreveu um papel do córtex cingulado em processos emocionais. Uma meta-análise recente de estudos em neuroimagem para identificação de processos emocionais mostrou ativações em porções rostrais do córtex cingulado anterior (CCA), dentre outras áreas (Kober *et al*., 2008). No quesito cognição, vários estudos têm detectado um papel do CCA na detecção de conflitos no processamento de informações (Cole *et al*., 2009). Também há muita associação do córtex cingulado, sobretudo em sua parte dorsal, com nocicepção (Vogt *et al*., 2003) (Figura 8).

Figura 8: funções atribuídas a regiões do córtex cingulado. À esquerda pontos de maior ativação em neuroimagem funcional relacionados a emoções, à direita pontos de ativação relacionados à estimulação nociceptiva térmica (obtido de Vogt *et al*., 2003).

Por ter sido implicado desde muito cedo como importante no entendimento das emoções, o córtex cingulado é uma das regiões de interesse mais pesquisadas em processos psicopatológicos. Alterações estruturais no córtex cingulado e também nos seus sulcos constituintes ou circundantes têm sido encontradas em várias patologias neuropsiquiátricas. Há evidências de diferenças volumétricas no córtex cingulado de pacientes com esquizofrenia (Noga *et al*., 1995; Kopelman *et al*., 2005; Fornito *et al*., 2009), transtorno bipolar (Atmaca *et al*., 2007; Fornito *et al*., 2009), depressão maior (Bora *et al*., 2012), transtorno obsessivo-compulsivo (Valente *et al*., 2005) e Alzheimer (Pengas *et al*., 2010), dentre outros. O estudo do córtex cingulado já trouxe ganhos importantes para pacientes com várias patologias neuropsiquiátricas, por exemplo o desenvolvimento de protocolo específico de localização de

estruturas cerebrais para a deep brain stimulation (DBS) para transtorno depressivo maior (Bora *et al*., 2012).

Merecem destaque alguns protocolos de segmentação manual, por serem os únicos a pôr em foco o córtex cingulado: os de McCormick *et al*. (2006), Jones *et al*. (2006) e Fornito *et al*. (2006). Embora haja controvérsias a respeito de subdivisões funcionais do córtex cingulado (Shackman *et al*. 2011), justifica-se a sua adoção, já que trabalhos recentes mostraram diferenças estruturais e/ou funcionais entre as subdivisões propostas por McCormick em determinadas patologias (Ichikawa *et al*., 2011; Gunning *et al*., 2009; Lindberg *et al*., 2009). O trabalho de Jones *et al*. (2006) é o único que traz regras mais claras para o parcelamento do córtex cingulado posterior (CCP), mas o foco principal do trabalho não é o protocolo.

5.3. DIFERENÇAS ENTRE OS PROTOCOLOS EXISTENTES NA LITERATURA E O DESTE TRABALHO.

O protocolo de McCormick *et al.* (2006) destaca-se por fazer uma revisão dos outros protocolos existentes, sobretudo o de Crespo-Facorro *et al.* (1999), diferenciando-se deste porque foca no cingulado anterior ao invés do lobo frontal como um todo. Ele também propõe subdivisões não utilizadas anteriormente, baseadas em estudos prévios de neuroimagem funcional que encontraram diferenças em áreas específicas ao longo do cíngulo anterior. As subdivisões propostas são quatro: subgenual, subcaloso, rostral e dorsal, e, para estabelecê-las, os autores utilizam um esquema de três planos verticais. O primeiro plano é traçado nas imagens coronais, um *slice* à frente do *genu* do corpo caloso, definindo o limite posterior do córtex cingulado anterior rostral e o limite anterior dos córtices subcaloso e rostral. O segundo plano é traçado também em *slices* coronais, no primeiro onde não é mais possível ver o putâmen entre os gânglios basais. O terceiro plano é discriminado nas imagens sagitais, como uma linha vertical através do meio do primeiro giro anterior a onde o ramo marginal conecta-se com o sulco cingulado.

Essas divisões do cíngulo anterior são mantidas no protocolo do presente trabalho, com uma diferença fundamental: o terceiro plano é colocado no ponto correspondente à coordenada Y = -10, representando o décimo *slice* coronal posterior à comissura anterior (no espaço estereotáxico padrão de Tailarach & Tournoux, 1988, a comissura anterior é o ponto X, Y, Z = 0). Existem duas razões básicas para essa mudança. A primeira é que a colocação de um marcador estereotáxico ao invés de um anatômico uniformiza a marcação entre os

cérebros, visto que há muitas diferenças anatômicas entre os indivíduos. A segunda é para justificar o porquê desse ponto ter sido escolhido: em 1976, Heiko Braak, um anatomista alemão, descobriu um campo celular gigantopiramidal primitivo no fundo do sulco cingulado, e o final desse campo corresponde aproximadamente ao ponto Y = -10. Células gigantopiramidais estão presentes nas áreas motoras pré-frontais. Na época da descoberta, Braak não dispunha da neuroimagem e o espaço estereotáxico padrão só viria a ser descrito em 1988 por Tailarach & Tournoux. Entretanto, no seu trabalho, Braak o descreve começando no plano da comissura anterior e terminando no dos corpos mamilares. Ocorre que o plano dos corpos mamilares, no atlas de Fonov *et al.* (2009), encontra-se no Y = -10. Logo, assume-se que tal marcador está relacionado ao fim da área motora do córtex cingulado.

Outra diferença importante em relação ao protocolo de McCormick *et al.* diz respeito à área subgenual. Enquanto McCormick *et al.* preferiram usar somente o plano relacionado ao putâmen para estabelecer o limite anterior da área subgenual, e não se importaram em incluir alguma porção do giro reto dentro dessa área; neste trabalho o sulco subcaloso anterior também é usado como limite anterior, quando presente, desta forma tentando retirar do córtex subgenual a maior parte do giro reto.

No trabalho de Fornito *et al.* (2006), encontramos regras bem descritas sobre como identificar os sulcos cingulado, paracingulado e superior rostral, as quais foram adaptadas no presente protocolo, especialmente as referentes ao sulco superior rostral e como proceder com suas variações. Fornito *et al.* não se ocuparam do córtex posterior e nem com o subgenual, mas as regras para o anterior, bem como suas subdivisões, são muito semelhantes às de McCormick *et al.*. Ressalta-se a controvérsia sobre a delimitação posterior do córtex cingulado anterior dorsal, que no protocolo de Fornito *et al.* é uma linha traçada no plano da comissura anterior, o que, segundo os autores, corresponde ao início da área motora do córtex cingulado. O foco do trabalho de Fornito *et al.* é, entretanto, o parcelamento manual e a diferenciação do córtex cingulado e do paracingulado.

Na literatura, o único estudo que traz regras mais detalhadas para a demarcação manual do córtex cingulado posterior em imagens de ressonância magnética é o de Jones *et al.* (2006). No entanto, o foco principal do trabalho não é o protocolo em si, mas o estudo de diferenças volumétricas no giro do cíngulo entre indivíduos com Alzheimer e controles. O marcador anatômico mais interessante de Jones *et al.* é o que separa o córtex cingulado posterior do córtex retroesplenial, também utilizado no presente protocolo. A principal diferença diz respeito à utilização do sulco esplenial como limite: Jones *et al.* preferiram evitar incluir a matéria cinzenta ao redor do sulco como parte do cíngulo posterior, pois ela é

constituída pela área histológica de Brodmann 31, a mesma presente nos lóbulos paraespleniais e, portanto, não exclusiva ao cíngulo. Entretanto, os próprios autores ressaltam que é muito difícil estabelecer o limite entre as áreas do cíngulo e as paraespleniais num nível macroscópico. Para tentar um grau de reprodutibilidade melhor, o fundo do sulco esplenial é utilizado como marcador no presente trabalho.

Nenhum dos três trabalhos, e nem outros protocolos que envolvam estruturas da região (Bonilha *et al.*, 2004), ocupou-se em delimitar a região, área ou lóbulo caudomedial. Essa estrutura foi descrita em mais detalhes por Vogt *et al.* (2001), e consiste na junção entre o córtex cingulado posterior com as áreas para-hipocampais. Ela estaria envolvida em tarefas envolvendo memória auditiva (Vogt *et al.*, 2001). A razão para não ser incluída em protocolos anteriores de forma separada provavelmente reside na dificuldade de seu parcelamento, e neste manual será feita uma tentativa de sua demarcação.

6. REFERÊNCIAS BIBLIOGRÁFICAS DA INTRODUÇÃO

Ashburner J. A fast diffeomorphic image registration algorithm. Neuroimage. 2007;38(1):95-113.

Ashburner J, Friston KJ. Spatial normalisation using basis functions. In: Frackowiak R, Friston KJ, Frith CD, Dolan RJ, Price CJ, Zeki S, Ashburner J et al., editores. Human Brain Function, 2a ed. Amsterdam: Elsevier; 2004. p. 655-672

Ashburner J, Friston KJ. Voxel-based morphometry – the methods. Neuroimage. 2000;11(6 Pt 1):805-21.

Atmaca M, Ozdemir H, Cetinkaya S, Parmaksiz S, Belli H, Poyraz AK, et al. Cingulate gyrus volumetry in drug free bipolar patients and patients treated with valproate or valproate and quetiapine. J Psychiatr Res. 2007;41(10):821-7.

Bergouignan L, Chupin M, Czechowska Y, Kinkingnéhun S, Lemogne C, Le Bastard G, et al. Can voxel based morphometry, manual segmentation and automated segmentation equally detect hippocampal volume differences in acute depression? Neuroimage. 2009;45(1):29-37.

Bonilha L, Kobayashi E, Cendes F, Min Li L. Protocol for volumetric segmentation of medial temporal structures using high-resolution 3-D magnetic resonance imaging. Hum Brain Mapp. 2004;22(2):145-54.

Bora E, Fornito A, Pantelis C, Yücel M. Gray matter abnormalities in Major Depressive Disorder: a meta-analysis of voxel based morphometry studies. J Affect Disord. 2012 Apr;138(1-2):9-18.

Braak H. A primitive gigantopyramidal field buried in the depth of the cingulate sulcus of the human brain. Brain Res. 1976;109(2):219-23.

Brett M, Christoff K, Cusack R, Lancaster J. Using the Talairach Atlas with the MNI Template. Neuroimage. 2001;13(6):S85

Cole MW, Yeung N, Freiwald WA, Botvinick M. Cingulate cortex: diverging data from humans and monkeys. Trends Neurosci. 2009;32(11):566-74.

Crespo-Facorro B, Kim JJ, Andreasen NC, O'Leary DS, Wiser AK, Bailey JM, et al. Human frontal cortex: an MRI-based parcellation method. Neuroimage. 1999;10(5):500-19.

Dale AM, Fischl B, Sereno MI. Cortical surface-based analysis. I. Segmentation and surface reconstruction. Neuroimage. 1999;9(2):179-94.

Damadian R. Tumor detection by nuclear magnetic resonance. Science. 1971;171(3976):1151-3.

Desikan RS, Ségonne F, Fischl B, Quinn BT, Dickerson BC, Blacker D, et al. An automated labeling system for subdividing the human cerebral cortex on MRI scans into gyral based regions of interest. Neuroimage. 2006 Jul 1;31(3):968-80.

Edelstein WA, Hutchison JM, Johnson G, Redpath T. Spin warp NMR imaging and applications to human whole-body imaging. Phys Med Biol. 1980;25(4):751-6.

Entis JJ, Doerga P, Barrett LF, Dickerson BC. A reliable protocol for the manual segmentation of the human amygdala and its subregions using ultra-high resolution MRI. Neuroimage. 2012;60(2):1226-35.

Ernst R. Gyromagnetic resonance fourier transform zeugmatography. US 4,070,611: United States Patent Office, 1978.

Filler A. The history, development and impact of computed imaging in neurological diagnosis and neurosurgery: CT, MRI, and DTI. 2009. Disponível em: http://precedings.nature.com/documents/3267/version/5

Fischl B, Salat DH, Busa E, Albert M, Dieterich M, Haselgrove C, et al. Whole brain segmentation: automated labeling of neuroanatomical structures in the human brain. Neuron. 2002;33(3):341-55.

Fischl B, Sereno MI, Dale AM. Cortical surface-based analysis. II: Inflation, flattening, and a surface-based coordinate system. Neuroimage. 1999;9(2):195-207.

Fischl B, van der Kouwe A, Destrieux C, Halgren E, Ségonne F, Salat DH, et al. Automatically parcellating the human cerebral cortex. Cereb Cortex. 2004;14(1):11-22.

Fonov VS, Evans AC, McKinstry RC, Almli CR and Collins DL. Unbiased nonlinear average age-appropriate brain templates from birth to adulthood. Neuroimage. 2009; 47, Suppl 1:S102. Organization for Human Brain Mapping 2009 Annual Meeting.

Fornito A, Whittle S, Wood SJ, Velakoulis D, Pantelis C, Yücel M. The influence of sulcal variability on morphometry of the human anterior cingulate and paracingulate cortex. Neuroimage. 2006;33(3):843-54.

Fornito A, Yücel M, Pantelis C. Reconciling neuroimaging and neuropathological findings in schizophrenia and bipolar disorder. Curr Opin Psychiatry. 2009;22(3):312-9.

Freud, S. Projeto para uma psicologia científica. 1895. In:_____ Edição standard brasileira das obras psicológicas completas. Tradução e direção de Jayme Salomão. 23 ed. Rio de Janeiro: Imago, 1974. v.1, p. 395-506.

Geuze E, Vermetten E, Bremner JD. MR-based in vivo hippocampal volumetrics: 1. Review of methodologies currently employed. Mol Psychiatry. 2005;10(2):147-59.

Good CD, Johnsrude IS, Ashburner J, Henson RN, Friston KJ, Frackowiak RS. A voxel-based morphometric study of ageing in 465 normal adult human brains. Neuroimage. 2001;14:21-36.

Gunning FM, Cheng J, Murphy CF, Kanellopoulos D, Acuna J, Hoptman MJ, et al. Anterior cingulate cortical volumes and treatment remission of geriatric depression. Int J Geriatr Psychiatry. 2009;24(8):829- 36.

Harris G, Andreasen NC, Cizadlo T, Bailey JM, Bockholt HJ, Magnotta VA, et al. Improving tissue classification in MRI: a three-dimensional multispectral discriminant analysis method with automated training class selection. J Comput Assist Tomogr. 1999;23(1):144-54.

Hayes K, Buist R, Vincent TJ, Thiessen JD, Zhang Y, Zhang H, et al. Comparison of manual and semi-automated segmentation methods to evaluate hippocampus volume in APP and PS1 transgenic mice obtained via in vivo magnetic resonance imaging. J Neurosci Methods. 2014;221:103-11.

Hendee WR, Morgan CJ. Magnetic resonance imaging. Part I – physical principles. West J Med. 1984;141(4):491-500.

Hoexter MQ, de Souza Duran FL, D'Alcante CC, Dougherty DD, Shavitt RG, Lopes AC, et al. Gray matter volumes in obsessive-compulsive disorder before and after fluoxetine or cognitive-behavior therapy: a randomized clinical trial. Neuropsychopharmacology. 2012;37(3):734-45.

Hyman SE. “Neural Science” [comentário]. In: Kandel ER. Psychiatry, Psychoanalysis and the New Biology of Mind. Washington, DC: American Psychiatric Publishing; 2005. p. 199-202.

Ichikawa N, Siegle GJ, Jones NP, Kamishima K, Thompson WK, Gross JJ, et al. Feeling bad about screwing up: emotion regulation and action monitoring in the anterior cingulate cortex. Cogn Affect Behav Neurosci. 2011;11(3):354-71.

Jones BF, Barnes J, Uylings HB, Fox NC, Frost C, Witter MP, et al. Differential regional atrophy of the cingulate gyrus in Alzheimer disease: a volumetric MRI study. Cereb Cortex. 2006;16(12):1701-8.

Kandel ER, Schwartz JH, Jessel TM. Principles of Neural Science. 4a ed. New York, NY: McGraw-Hill; 2000.

Kandel ER, Squire LR. Neuroscience: breaking down scientific barriers to the study of brain and mind. Science. 2000;290(5494):1113-20.

Kober H, Barrett LF, Joseph J, Bliss-Moreau E, Lindquist K, Wager TD. Functional grouping and cortical-subcortical interactions in emotion: a meta-analysis of neuroimaging studies. 2008;42:998–1031.

Kopelman A, Andreasen NC, Nopoulos P. Morphology of the anterior cingulate gyrus in patients with schizophrenia: relationship to typical neuroleptic exposure. Am J Psychiatry. 2005;162(10):1872-8.

Lauterbur PC. Image formation by induced local interactions: examples employing nuclear magnetic resonance. Nature 1973;242:190–191.

Li DF, Freeman AW, Tran-Dinh H, Morris JG. A Cartesian coordinate system for human cerebral cortex. J Neurosci Methods. 2003;125(1-2):137-45.

Lindberg O, Ostberg P, Zandbelt BB, Oberg J, Zhang Y, Andersen C, et al. Cortical morphometric subclassification of frontotemporal lobar degeneration. AJNR Am J Neuroradiol. 2009;30(6):1233-9.

McCormick LM, Ziebell S, Nopoulos P, Cassell M, Andreasen NC, Brumm M. Anterior cingulate cortex: an MRI-based parcellation method. Neuroimage. 2006;32(3):1167-75.

Noga JT, Aylward E, Barta PE, Pearlson GD. Cingulate gyrus in schizophrenic patients and normal volunteers. Psychiatry Res. 1995;61(4):201-8.

Oguz I, Sonka M. LOGISMOS-B: Layered Optimal Graph Image Segmentation of Multiple Objects and Surfaces for the Brain. IEEE Trans Med Imaging. 2014 Feb 7. [publicação eletrônica] doi: 10.1109/TMI.2014.2304499

Paus T. Primate anterior cingulate cortex: where motor control, drive and cognition interface. Nat Rev Neurosci. 2001;2(6):417-24.

Pengas G, Hodges JR, Watson P, Nestor PJ. Focal posterior cingulate atrophy in incipient Alzheimer's disease. Neurobiol Aging. 2010;31(1):25-33.

Pykett IL, Newhouse JH, Buonanno FS, Brady TJ, Goldman MR, Kistler JP, et al. Principles of nuclear magnetic resonance imaging. Radiology. 1982;143(1):157-68.

Ranta ME, Crocetti D, Clauss JA, Kraut MA, Mostofsky SH, Kaufmann WE. Manual MRI parcellation of the frontal lobe. Psychiatry Res. 2009;172(2):147-54.

Salat DH, Lee SY, van der Kouwe AJ, Greve DN, Fischl B, Rosas HD. Age-associated alterations in cortical gray and white matter signal intensity and gray to white matter contrast. Neuroimage. 2009;48(1):21-8.

Scherzinger AL, Hendee WR. Basic principles of magnetic resonance imaging – an update. West J Med. 1985;143(6):782-92.

Shackman AJ, Salomons TV, Slagter HA, Fox AS, Winter JJ, Davidson RJ. The integration of negative affect, pain and cognitive control in the cingulate cortex. Nat Rev Neurosci. 2011;12(3):154-67.

Talairach J, Tournoux P. Co-Planar Stereotaxic Atlas of the Human Brain. Stuttgart: Georg Thieme Verlag; 1988.

Valente AA Jr, Miguel EC, Castro CC, Amaro E Jr, Duran FL, Buchpiguel CA, et al. Regional gray matter abnormalities in obsessive-compulsive disorder: a voxel-based morphometry study. Biol Psychiatry. 2005;58(6):479-87.

Valenzuela M, Bartrés-Faz D, Beg F, Fornito A, Merlo-Pich E, Müller U, et al. Neuroimaging as endpoints in clinical trials: Are we there yet? Perspective from the first Provence workshop. Mol Psychiatry. 2011;16(11):1064-6.

Vogt BA, Berger GR, Derbyshire SW. Structural and functional dichotomy of human midcingulate cortex. Eur JNeurosci 2003;18:3134-3144.

Vogt BA, Hof PR, Vogt LJ. Cingulate gyrus. In: Paxinos G, Mai JK, editores. The human nervous system. San Diego, CA: Academic Press; 2004. p 915-949.

Vogt BA, Vogt LJ, Perl DP, Hof PR. Cytology of human caudomedial cingulate, retrosplenial, and caudal parahippocampal cortices. J Comp Neurol. 2001;438(3):353- 76.

7. OBJETIVO

Criar e testar a reproducibilidade de um novo protocolo de parcelamento de todo o córtex cingulado em ressonância magnética, levando em conta novas demarcações mais baseadas em critérios histológicos e anatômicos não considerados previamente, como o sulco subcaloso anterior, o campo gigantopiramidal de Braak e a área caudomedial.

8. ARTIGO CIENTÍFICO EM INGLÊS A SER SUBMETIDO PARA A REVISTA *PSYCHIATRY RESEARCH: NEUROIMAGING*

THE CINGULATE CORTEX AND ITS SUBDIVISIONS: MANUAL PARCELLATION PROTOCOL IN MAGNETIC RESONANCE IMAGING

Authors: Thiago Casarin Hartmann[1], Paola Bell Felix de Oliveira[1], Daniel Luccas Arenas[1], João Pedro Sanvitto[2], Tom Beaudry[3], Pedro Rosa-Neto[3], Ygor Arzeno Ferrão[1]

[1] Universidade Federal de Ciências da Saúde de Porto Alegre

[2] Pontifícia Universidade Católica de Porto Alegre

[3] McGill University, Montreal, QC, Canada

Corresponding author:

Thiago Casarin Hartmann

Rua Tentente Ary Tarrago, 1720, casa 58, Protásio Alves

Porto Alegre, RS, Brazil. CEP 91225-001

Phone: +55 (51) 9913-5733

E-mail: hartmann321@yahoo.com.br

ABSTRACT

The cingulate gyrus has a central role in most theories of emotions and is associated with several neuropsychiatric disorders, for instance amnestic mild cognitive impairment (aMCI). One of the most used techniques in neuroimaging studies is the analysis of regions of interest by manual parcellation on magnetic resonance images (MRI). There are many manual parcellation protocols for regions of the cingulate gyrus, but there is no consensus of the best way to do it. This study aimed to develop a reliable MRI parcellation protocol of the entire cingulate cortex, adapting and standardizing existing methods, with the addition of landmarks hitherto not considered. Three raters tested its replicability in 8 MRIs from brains of aMCI patients and controls. The software used was Display for Linux, which permits the parcellation of regions of interest with simultaneous interactive visualization of all axes. A cingulate cortex 7 regions division for each hemisphere was proposed and a new stereotaxic landmark was delineated for the border between the anterior and posterior cingulate cortices. The intraclass correlation coefficients were satisfactory for most regions. Results were better for larger regions. Probabilistic maps were generated to evaluate concordant regions.

Keywords: cingulate cortex, parcellation, MRI, volumetrics, cingulate gyrus.

1. Introduction

The cingulate gyrus is the most prominent cortical structure in the medial surface of the human brain. It forms a belt extending from the lamina terminalis, rostral to the anterior commissure, encircling the corpus callosum and ending just ventral to the splenium of corpus callosum. The cingulate gyrus forms the dorsal component of the grand limbic lobe of Broca (1878 apud Vogt *et al*., 2004) and has a central role in most theories of emotions. The most classical subdivision of its cortical region encompasses the anterior cingulate cortex, the posterior cingulate cortex and the retrosplenial cortex (Vogt *et al*., 2004).

The cingulate cortex is seen as an integrator of emotional and cognitive responses (Shackman *et al*., 2011; Paus T, 2001). Papez (1937 apud Shackman et al., 2011), in a seminal work, described a role of the cingulate cortex in emotional processes. A meta-analysis of neuroimaging studies to identify cortical areas associated with emotions showed activations in rostral portions of the anterior cingulate cortex (ACC), among other areas (Kober *et al*., 2008). On the issue of cognition, several studies have demonstrated a role of the ACC in detecting conflicts in information processing (Cole *et al*., 2009). There is also a lot of association between the cingulate cortex and nociception, particularly in its dorsal part (Vogt *et al*., 2003).

Currently, neuroimaging is able to reveal an extraordinary amount of information about the structural, functional and biochemical characteristics of the human brain. Moreover, some authors have advocated the use of neuroimaging outcomes for clinical trials (Valenzuela *et al*., 2011; Hoexter *et al*., 2011). There is a wide range of techniques applied on neuroimaging to study determined brain regions. Two groups of techniques are used to detect structural abnormalities: regions of interest (region-of-interest – ROI) or whole brain analysis. The first type involves the delineation of desired brain structure according to anatomical criteria pre-established by protocols, and in the second case the most used technique is voxel-based morphometry (VBM), an automated technique that enables quick comparisons involving the entire brain. However, the results found by VBM can also be attributed to differences in brain form of each individual (Fornito *et al*., 2009). Therefore, although with important limitations, the manual segmentation techniques are still considered the gold standard for studying macro-regions and / or areas of difficult separation between white and gray matter, such as the hippocampus (Bergouignan *et al*., 2009; Bora *et al*., 2012; Geuze *et al*. 2005; Hayes *et al*., 2014).

For its early discovered importance on understanding emotions, the cingulate cortex is one of the most researched ROI in psychopathological processes. Structural changes in the

cingulate cortex and also in its constituent or surrounding sulci have been found in several neuropsychiatric disorders. There are evidences of volumetric differences in cingulate cortex of patients with schizophrenia (Noga *et al*., 1995, Kopelman *et al*., 2005, Fornito *et al*., 2009), bipolar disorder (Atmaca *et al*., 2007, Fornito *et al*., 2009), major depression (Bora *et al*., 2012), obsessive-compulsive disorder (Valente *et al*., 2005), Alzheimer (Pengas *et al*., 2010) and amnestic mild cognitive impairment (Han *et al.*, 2012, Zhao *et al.*, 2014), among others.

There are several manual parcellation protocols of regions of the cingulate cortex in the literature. The following three are the most recent and widely used for their good reliability and reproducibility: McCormick *et al*. (2006), Jones *et al*. (2006), and Fornito *et al*. (2006). The first occupies itself only of the anterior cingulate. The latter involves the division of the paracingulate cortex, but it also has rules only for the anterior cingulate. Jones *et al*. (2006) bring clearer rules for the parcellation of the posterior cingulate cortex, but the main focus of the paper is not the parcellation protocol. Moreover, it excludes the subgenual cortex and the caudomedial region. Although there is controversy regarding the functional subdivisions of the cingulate cortex (Shackman *et al*., 2011), recent studies have shown structural and/or functional differences between the anterior cingulate subdivisions proposed by McCormick in certain pathologies (Ichikawa *et al*., 2011; Gunning *et al*., 2009; Lindberg *et al*., 2009). So far, no work has proposed to create a valid method of parcellation of the entire cingulate cortex, with the segmentation of all its subdivisions. There is considerable controversy among the aforementioned protocols concerning the delimitation of the boundary between subareas, particularly the anterior and posterior parts.

The purpose of the present research is the creation of a new method of segmentation of the entire cingulate cortex, adapting and standardizing existing protocols. In addition, its inter-rater reproducibility is tested. The most important innovations of this new protocol are described hereafter. A new way to separate the anterior and posterior cingulate cortices is presented: a stereotaxic marker corresponding approximately to the end of the motor cingulate area delineated by Paus *et al*. (1996b), and the end of the Braak's gigantopiramidal field (1976) (Paus T., 2001). An attempt to delineate the caudomedial region was also done. The caudomedial region is the point where the cingulate Brodmann's areas (23a and 23b) and retrosplenial areas (29 and 30) border the parahippocampal areas (27, 36 and 36’). Although this region has histological parts related to the cingulate cortex, it is often removed from the parcellation protocols because of its difficult demarcation (Vogt *et al*., 1995; Vogt *et al*., 2001). Recent considerations about the anatomy of subcallosal area also were taken into account (Spasojevic *et al*., 2011).

2. Methods

2.1. Sample:

Magnetic resonance images (MRIs) were obtained from a sample of patients with amnestic type mild cognitive impairment, diagnosed using the Petersen criteria (Petersen, 2004), and healthy controls matched for age. The sample belongs to a database pool of the McGill Centre for Studies in Aging (MCSA) (McGill University, Montreal, QC, Canada). This sample was chosen to avoid new subject recruitment, as it is part of another study (Wu *et al.*, 2014). Patients and controls were recruited by a neurologist expert in dementia. A total of 8 MRIs randomly chosen from the database were used for this preliminary study. No MRI presented with major structural alterations, such as tumors, demyelination or agenesis. Every subject who was scanned (or his/her legal responsible) first gave written informed consent. This study and the original one which gave origin to the database pool were approved by the local ethics committees.

2.2. MRI acquisition parameters:

Structural and functional sequences were obtained on a 3.0T Siemens MAGNETOM Trio system using a 32-channel coil. Foam pads and headphones were used to reduce the mobility of the head and the noise of the scanner. MRIs used were high-resolution anatomical images acquired in T1 with the following parameters: TR/TE=23 ms/29 ms, 256x256 matrix with a resolution of 1x1 mm^3, 176 contiguous sagittal sections covering the whole brain, inclination angle=90°.

2.3. Image processing prior to manual parcellation:

Different algorithms from the McConnell Brain Imaging Centre (Montreal, Canada) were used to prepare raw MRI volumes. First, raw images were converted into the “minc” electronic file format (see http://www.bic.mni.mcgill.ca/software/minc/minc.html). Second, images were automatically registered into stereotaxic space (Talairach and Tornoux, 1988) to adjust for differences in brain volume and orientation and to minimize variability in slice orientation (Collins *et al.*, 1994; Lancaster *et al.*, 1995; Paus *et al.*, 1996a; Penhune *et al.*, 1996). Third, images were corrected for field nonuniformity using the N3 software program (online at http://www.bic.mni.mcgill.ca/software/N3/) (Sled *et al.*, 1998). The T1 was classified into grey matter (GM), white matter (WM), and cerebrospinal fluid (CSF) with the INSECT algorithm (Zijdenbos *et al.*, 1998). The analytic pipeline is demonstrated in figure 1.

INSERT FIGURE 1

2.4. Volumetric analysis:

The interactive software Display for Linux, developed by David McDonald at the Brain Imaging Centre of the Montreal Neurological Institute (McGill University, Montreal, QC, Canada) was used to manual delineate the ROIs. This software is a part of the minctools software package. It enables the interactive visualization of the three planes (sagittal, coronal and axial); the manual demarcation of interest areas; automatic segmentation of white matter, gray matter or cerebrospinal fluid using predefined masks, and the automatic calculation of specific region volume.

2.5. The manual parcellation protocol:

A more detailed version of the protocol is attached to the end, here are summarized the subregions main landmarks. In the full version there is also a sulci identification guide and a Display basic commands manual. After each subsection, one image is shown with the parcellated region, and in the end a whole parcellated cingulate cortex is depicted.

2.5.1. Subgenual cortex (SGC):

The SGC rostral boundaries were the anterior subcallosal sulcus (ascs) and the most rostral coronal slice where the putamen appears, the latter in its dorsal part. The caudal boundary was the posterior subcallosal sulcus (pscs), the dorsal was the rostrum of the corpus callosum (cc) and the ventral was given by the merging of anterior and posterior subcallosal sulci, separating the SGC from the gyrus rectus. The parcellation followed a rostro-caudal direction on the coronal slices, always correcting itself by the medial sagittal ones, as one could see better the anatomic landmarks in the latter, but the cortex depth in the first.

INSERT FIGURE 2

2.5.2. Subcallosal anterior cingulate cortex (sACC):

The ventral-posterior border of sACC was the most caudal coronal slice before the putamen appears. This corresponded well with the point of transition between the horizontally oriented subcallosal continuation of the cingulate gyrus and the beginning of the more vertical cytoarchitectural area of the paraterminal gyrus (McCormick *et al*., 2006). The cingulate

cortex limits were set in the cingulate sulcus (cgs) fundus (inferior), or superior rostral sulcus (srs) fundus when the cgs merged with it or ended before it, and at the edge of the callosal sulcus (cas) dorsal bank (superior). The sACC parcellation was performed mainly on the coronal slices.

INSERT FIGURE 3

2.5.3. Rostral anterior cingulate cortex (rACC):

The first coronal slice marking the beginning of the rACC was one forward from the slice in which the two sides of the cc were no longer connected through the genu. The limits were set in the fundus of the ventral and dorsal cingulate sulci (above and below the cc, in the coronal view).

INSERT FIGURE 4

2.5.4. Dorsal anterior cingulate cortex (dACC):

The region caudal to the first coronal slice where the two sides of the cc were no longer connected through the genu until the Y = -10 coronal slice, dorsally to corpus callosum, was the dorsal anterior cingulate cortex (dACC). The cortical area between the cas ventral bank edge and the cgs fundus was parcellated.

INSERT FIGURE 5

2.5.5. Posterior cingulate cortex (PCC) and retrosplenial cortex (RSC):

The PCC parcellation followed the dACC orientation, starting at the Y = -10 coronal slice. However, the PCC ventral limit was the cas dorsal bank edge instead of its ventral bank, because the cortex surrounding the cas was the RSC (Jones *et al*., 2006). Caudally to the marginal ramus (mr), the dorsocaudal limit of the PCC became the splenial sulcus (spls). The ventral caudal border of PCC was set on the most ventral axial slice on which the curvature of the splenium of the cc was visible.

INSERT FIGURE 6

2.5.6. Caudomedial region (CMR):

The CMR lateral limit was the most lateral sagittal slice in which it was still possible to see CSF inside the whole extension of the anterior calcarine sulcus (acals). The majority of our sample showed the acals interruption in its most rostral part, but sometimes it was interrupted more caudally.

The CMR parcellation followed a latero-medial orientation through sagittal slices. Its ventro-caudal limit was given by the acals, and, as the parcellation proceeded dorsally, by the same caudal limit set for the PCC end. The dorsal limit was the the first axial slice where the cc two sides were no longer connected through the splenium, i.e., the end of PCC + RSC. The rostral limit was the small stripe of CSF behind the thalamic pulvinar nucleus.

INSERT FIGURES 7 & 8

2.6. Reproducibility:

One rater (T.H.) performed the parcellation prior to others while developing the protocol. After this first protocol application, two other raters (J.S. and P.O.) were trained in order to test the inter-rater reliability. Following the training procedure, which consisted in basic commands in the Display software, both raters independently parcellated the same set of MRIs used by the first rater (T.H.).

2.7. Statistical analysis:

The three raters Intraclass Correlation Coefficient (ICC) was calculated for the volumes of each cingulate subregion and the total for the left and right cingulate cortices. A mean volume of each region was also calculated. A Spearman correlation between the ICC value and the mean volumes was performed to evaluate if the size of the subregion influenced in the reliability of its parcellation. Shapiro-Wilk's test was conducted to investigate if the data were normally distributed. The level of statistical significance (alpha) was 5%. Statistical calculations were conducted using SPSS v20.0.0 for Mac. The volumes were calculated using the Display program.

After the manual parcellation, probabilistic maps were generated with binarized labeled images using the register software. The register software is also a part of the minctools software package.
(see http://www.bic.mni.mcgill.ca/ServicesSoftwareVisualization/HomePage)

3. Results

Table 1 shows the pooled mean volumes for each region, as parcellated by the three raters.

INSERT TABLE 1

The ICCs for each region are displayed in the table 2.

INSERT TABLE 2

The Spearman's correlation between the ICCs and the mean volumes was r = 0.67 (p = 0.005), which means that the higher the structure volume the higher reliability was achieved in its parcellation.

The probabilistic maps are portrayed in the figure 9. Less reproducible regions occurred in the limits shown on the map.

INSERT FIGURE 9

4. Discussion

This study presents the inter-rater reliability of a new method for parcellating the cingulate cortex as a whole in MRI. The protocol used was adapted mainly from the previous works by McCormick *et al*. (2006) regarding the ACC parcellation and Jones *et al*. (2006), regarding the PCC. The subdivisions proposed by McCormick *et al*. (2006) proved to be worthy, since more recent papers found important differences among them (Ichikawa *et a*l., 2011; Gunning *et al*., 2009; Lindberg *et al*., 2009). The most profound difference between the present and the cited protocols was a new stereotaxic marker for the delimitation of the anterior/posterior boundary, which was Y = -10. That landmark suits well with the end of the caudal cingulate motor area (Paus *et al*., 1996b). Also, it sets the end of the gigantopyramidal field of Braak (Braak H., 1976). The avoiding of an anatomical landmark in this situation could have accounted for better ICCs between the raters, since there is no doubt about where is the Y = -10 slice. In fact, for the dACC the present ICCs were better than those achieved by McCormick *et al*. (2006) (left = 0.98 and right = 0.99 vs. left = 0.91 and right = 0.85). Other differences between the landmarks involved the SGC, as recent considerations about the anatomy of this region were taken into account (Spasojevic *et al*., 2011). For instance, a detailed description of the morphology of the ascs is given in the sulci identification guide,

and an attempt to use this sulcus as an anatomical landmark was also driven. This sulcus is highly variable across multiple individuals (Spasojevic *et al*., 2011; Ono *et al*., 1990) and perhaps this was the main reason for the poorer ICC of this region in contrast with McCormick *et al*. (2006) previous results (left = 0.53 and right = 0.56 vs. left = 0.86 and right = 0.85).

Another important difference between the present work and the others is the fact that this is the first attempt in the literature to parcellate the CMR in MRI. Vogt *et al*. (2001) describe this area in histological details, also naming it caudomedial lobule when the common trunk between the parieto-occipital and calcarine sulci (acals) clearly forms a lobule. Our whole sample presented with the acals, but still we thought it was better to keep the name region instead of lobule because it would account for cases without a clear lobule form as well. This region is very small and difficult to parcellate, as evidenced by its ICC results. Jones *et al*. (2006) carefully avoided this area, arguing that maintaining the PCC parcellation always dorsal to the cc splenium ensures that no parahippocampal cortices are pick. However, there is a need to at least focus attention on the CMR, since it has many interconnections with PCC, SGC and RSC, that subserve memory and visuospatial functions (Vogt *et al*., 2004).

The PCC and RSC parcellation followed mainly the landmarks set by Jones *et al*. (2006), as mentioned above. However, even though they preferred to avoid segmenting Brodmann area 31 (which surrounds the spls), they also stated that it is difficult to set its limits in a macroscopical level. For reliability purposes, the PCC dorsal limit was defined in this protocol as the spls fundus. Nevertheless, an attempt was made to keep the parcellation as close as possible to the cc, in order to minimize the inclusion of the aforementioned area. The ICCs for the RSC differed substantially from Jones *et al*. (2006). One possible reason could have been that they tested its inter-rater reliability without separating it from the PCC, minimizing the RSC small size effect in this way. Once again, the separation between these two cortices is recommended, as they have important histological and functional differences that may false functional neuroimaging studies (Vogt *et al*., 2001; Vogt *et al*., 2004).

Probabilistic maps of the binarized images of parcellated cingulate cortices were generated in order to identify the regions where the correlation between raters were better. They consist in a 3D image of the likelihood that any voxel will be labeled as including the ROI. Thus, superimposing the parcellation of each rater, it is possible to visualize the areas with better and worse inter-rater correlations. Probabilistic maps are used for several finalities: localizing peak cortical activations in the stereotaxic space during cognitive task performances, for instance (Paus *et al*., 1996a). In the present study they are used only for

visualization purposes. According to the maps, the worst correlations were achieved in peripheral areas. This must be taken into account in future directions of the protocol improvement for better ICCs. No protocol cited have used probabilistic maps to visualize raters correlations.

This study has some limitations that need to be mentioned. First, the small sample may false the results, since there is high variability in the medial surface of the human brain hemispheres (Ono *et al*., 1990; Vogt *et al*., 1995; Crespo-Facorro *et al*., 1999). Still, the majority of protocols seldom used more than 25 MRIs for reliability assessment (Crespo-Facorro *et al*., 1999; Bonilha *et al*., 2004; McCormick *et al*., 2006; Jones *et al*., 2006; Fornito *et al*., 2006; Ranta *et al*., 2009). Second, the present protocol did not consider the parcellation of the paracingulate cortex, as proposed by Fornito *et al*. (2006), for two reasons: a) to improve reliability and, b) because the protocol by McCormick *et al*. (2006) also did not and has been proved worthy (Ichikawa *et al*., 2011; Gunning *et al*., 2009; Lindberg *et al*., 2009). Third, there is no intra-rater reliability assessment in this study.

The aim of the present study was to introduce a new method for the whole cingulate cortex manual parcellation, with a more satisfactory balance between inter-rater reliability and histological correlates among the subregions. As a whole, the reliability analysis showed a good ICC, although the smaller areas still need improvement. The modification of landmarks for these areas should be considered in order to optimize their reliability, but the present protocol can be readily used for the wider regions or for the whole cingulate cortex. The new anterior/posterior division landmark of Y = -10 is of easy application and has an approximate localization to the end of the cingulate motor area, thus making its use recommended.

References

Atmaca, M., Ozdemir, H., Cetinkaya, S., Parmaksiz, S., Belli, H., Poyraz, A.K., Tezcan, E., Ogur, E., 2007. Cingulate gyrus volumetry in drug free bipolar patients and patients treated with valproate or valproate and quetiapine. Journal of Psychiatric Research 41(10), 821-827.

Bergouignan, L., Chupin, M., Czechowska, Y., Kinkingnéhun, S., Lemogne, C., Le Bastard, G., Lepage, M., Garnero, L., Colliot, O., Fossati, P., 2009. Can voxel based morphometry, manual segmentation and automated segmentation equally detect hippocampal volume differences in acute depression? Neuroimage 45(1), 29-37.

Bonilha, L., Kobayashi, E., Cendes, F., Min Li, L., 2004. Protocol for volumetric segmentation of medial temporal structures using high-resolution 3-D magnetic resonance imaging. Human Brain Mapping 22(2), 145-154.

Bora, E., Fornito, A., Pantelis, C., Yücel, M., 2012. Gray matter abnormalities in Major Depressive Disorder: a meta-analysis of voxel based morphometry studies. Journal of Affective Disorders 138(1-2), 9-18.

Braak, H., 1976. A primitive gigantopyramidal field buried in the depth of the cingulate sulcus of the human brain. Brain Research 109(2), 219-223.

Cole, M.W., Yeung, N., Freiwald, W.A., Botvinick, M., 2009. Cingulate cortex: diverging data from humans and monkeys. Trends in Neurosciences 32(11), 566-574.

Collins, D.L., Neelin, P., Peters, T.M., Evans, A.C., 1994. Automatic 3-D inter-subject registration of MR volumetric data in standardized Talairach space. Journal of Computer Assisted Tomography 18, 192-205.

Crespo-Facorro, B., Kim, J.J., Andreasen, N.C., O'Leary, D.S., Wiser, A.K., Bailey, J.M., Harris, G., Magnotta, V.A., 1999. Human frontal cortex: an MRI-based parcellation method. Neuroimage 10(5), 500-519.

Fonov, V.S., Evans, A.C., McKinstry, R.C., Almli, C.R., Collins, D.L., 2009. Unbiased nonlinear average age-appropriate brain templates from birth to adulthood. Neuroimage 47, Supplement 1, S102. Organization for Human Brain Mapping 2009 Annual Meeting.

Fornito, A., Whittle, S., Wood, S.J., Velakoulis, D., Pantelis, C., Yücel, M., 2006. The influence of sulcal variability on morphometry of the human anterior cingulate and paracingulate cortex. Neuroimage 33(3), 843-854.

Fornito, A., Yücel, M., Pantelis, C., 2009. Reconciling neuroimaging and neuropathological findings in schizophrenia and bipolar disorder. Current Opinion in Psychiatry 22(3), 312-319.

Geuze, E., Vermetten, E., Bremner, J.D., 2005. MR-based in vivo hippocampal volumetrics: 1. Review of methodologies currently employed. Molecular Psychiatry 10(2), 147-159.

Gunning, F.M., Cheng, J., Murphy, C.F., Kanellopoulos, D., Acuna, J., Hoptman, M.J., Klimstra, S., Morimoto, S., Weinberg, J., Alexopoulos, G.S., 2009. Anterior cingulate cortical volumes and treatment remission of geriatric depression. International Journal of Geriatric Psychiatry 24(8), 829-836.

Han, Y., Lui, S., Kuang, W., Lang, Q., Zou, L., Jia, J., 2012. Anatomical and functional deficits in patients with amnestic mild cognitive impairment. PLoS One 7(2), e28664. doi: 10.1371/journal.pone.0028664.

Hayes, K., Buist, R., Vincent, T.J., Thiessen, J.D., Zhang, Y., Zhang, H., Wang, J., Summers, A.R., Kong, J., Li, X.M., Martin, M., 2014. Comparison of manual and semi-automated segmentation methods to evaluate hippocampus volume in APP and PS1 transgenic mice obtained via in vivo magnetic resonance imaging. Journal of Neuroscience Methods 221, 103-111.

Hoexter, M.Q., de Souza Duran, F.L., D'Alcante, C.C., Dougherty, D.D., Shavitt, R.G., Lopes, A.C., Diniz, J.B., Deckersbach, T., Batistuzzo, M.C., Bressan, R.A., Miguel, E.C., Busatto, G.F., 2012. Gray matter volumes in obsessive-compulsive disorder before and after fluoxetine or cognitive-behavior therapy: a randomized clinical trial. Neuropsychopharmacology 37(3), 734-745.

Ichikawa, N., Siegle, G.J., Jones, N.P., Kamishima, K., Thompson, W.K., Gross, J.J., Ohira, H., 2011. Feeling bad about screwing up: emotion regulation and action monitoring in the anterior cingulate cortex. Cognitive, Affective & Behavioral Neuroscience 11(3), 354-371.

Jones, B.F., Barnes, J., Uylings, H.B., Fox, N.C., Frost, C., Witter, M.P., Scheltens, P., 2006. Differential regional atrophy of the cingulate gyrus in Alzheimer disease: a volumetric MRI study. Cerebral Cortex 16(12), 1701-1708.

Kober, H., Barrett, L.F., Joseph, J., Bliss-Moreau, E., Lindquist, K., Wager, T.D., 2008. Functional grouping and cortical-subcortical interactions in emotion: a meta-analysis of neuroimaging studies. Neuroimage 42, 998-1031.

Kopelman, A., Andreasen, N.C., Nopoulos, P., 2005. Morphology of the anterior cingulate gyrus in patients with schizophrenia: relationship to typical neuroleptic exposure. The American Journal of Psychiatry 162(10), 1872-1878.

Lancaster, J.L., Glass, T.G., Lankipalli, B.R., Downs, H., Mayberg, H., Fox, P.T., 1995. A modality independent approach to spatial normalization of tomographic images of the human brain. Human Brain Mapping 3, 209-223.

Lindberg, O., Ostberg, P., Zandbelt, B.B., Oberg, J., Zhang, Y., Andersen, C., Looi, J.C., Bogdanović, N., Wahlund, L.O., 2009. Cortical morphometric subclassification of frontotemporal lobar degeneration. AJNR American Journal of Neuroradiology 30(6), 1233-1239.

McCormick, L.M., Ziebell, S., Nopoulos, P., Cassell, M., Andreasen, N.C., Brumm, M., 2006. Anterior cingulate cortex: an MRI-based parcellation method. Neuroimage 32(3), 1167-1175.

Noga, J.T., Aylward, E., Barta, P.E., Pearlson, G.D., 1995. Cingulate gyrus in schizophrenic patients and normal volunteers. Psychiatry Research 61(4), 201-208.

Ono, M., Kubick, S., Abernathey, C.D., 1990. Atlas of the Cerebral Sulci. Thieme, New York.

Paus, T., Otaky, N., Caramanos, Z., MacDonald, D., Zijdenbos, A., D'Avirro, D., Gutmans, D., Holmes, C., Tomaiuolo, F., Evans, A.C., 1996a. In vivo morphometry of the intrasulcal gray matter in the human cingulate, paracingulate, and superior-rostral sulci: hemispheric asymmetries, gender differences and probability maps. The Journal of Comparative Neurology 376, 664-673.

Paus T., 2001. Primate anterior cingulate cortex: where motor control, drive and cognition interface. Nature Reviews. Neuroscience 2(6), 417-424.

Paus, T., Tomaiuolo, F., Otaky, N., MacDonald, D., Petrides, M., Atlas, J., Morris, R., Evans, A.C., 1996b. Human cingulate and paracingulate sulci: pattern, variability, asymmetry, and probabilistic map. Cerebral Cortex 6(2), 207-214.

Pengas, G., Hodges, J.R., Watson, P., Nestor, P.J., 2010. Focal posterior cingulate atrophy in incipient Alzheimer's disease. Neurobiology of Aging 31(1), 25-33.

Penhune, V.B., Zatorre, R.J., MacDonald, J.D., Evans, A.C., 1996. Interhemispheric anatomical differences in human primary auditory cortex: probabilistic mapping and volume measurement from magnetic resonance scans. Cerebral Cortex 6, 661-672.

Petersen, R.C., 2004. Mild cognitive impairment as a diagnostic entity. Journal of Internal Medicine 256, 183-194.

Ranta, M.E., Crocetti, D., Clauss, J.A., Kraut, M.A., Mostofsky, S.H., Kaufmann, W.E., 2009. Manual MRI parcellation of the frontal lobe. Psychiatry Research 172(2), 147-154.

Shackman, A.J., Salomons, T.V., Slagter, H.A., Fox, A.S., Winter, J.J., Davidson, R.J., 2011. The integration of negative affect, pain and cognitive control in the cingulate cortex. Nature Reviews. Neuroscience 12(3), 154-167.

Sled, J.G., Zijdenbos, A.P., Evans, A.C., 1998. A nonparametric method for automatic correction of intensity nonuniformity in MRI data. IEEE Transactions on Medical Imaging 17, 87-97.

Spasojević, G.D., Malobabić, S., Suščević, D., Stijak, L., Nikolić, V., Gojković, I., 2011. Morphological variability of the subcallosal area of man. Surgical and Radiologic Anatomy 33(4), 313-318.

Talairach, J., Tournoux, P., 1988. Co-Planar Stereotaxic Atlas of the Human Brain. Georg Thieme Verlag, Stuttgart.

Valente, A.A. Jr., Miguel, E.C., Castro, C.C., Amaro, E. Jr., Duran, F.L., Buchpiguel, C.A., Chitnis, X., McGuire, P.K., Busatto, G.F., 2005. Regional gray matter abnormalities in obsessive-compulsive disorder: a voxel-based morphometry study. Biological Psychiatry 58(6), 479-487.

Valenzuela, M., Bartrés-Faz, D., Beg, F., Fornito, A., Merlo-Pich, E., Müller, U., Öngür, D., Toga, A.W., Yücel, M., 2011. Neuroimaging as endpoints in clinical trials: Are we there yet? Perspective from the first Provence workshop. Molecular Psychiatry 16(11), 1064-1066.

Vogt, B.A., Berger, G.R., Derbyshire, S.W., 2003. Structural and functional dichotomy of human midcingulate cortex. The European Journal of Neuroscience 18, 3134-3144.

Vogt, B.A., Hof, P.R., Vogt, L.J., 2004. Cingulate gyrus. In: Paxinos, G., Mai, J.K. (Eds.), The human nervous system. Academic Press, San Diego. pp. 915-949.

Vogt, B.A., Nimchinsky, E.A., Vogt, L.J., Hof, P.R., 1995. Human cingulate cortex: surface features, flat maps, and cytoarchitecture. The Journal of Comparative Neurology 359(3), 490-506.

Vogt, B.A., Vogt, L.J., Perl, D.P., Hof, P.R., 2001. Cytology of human caudomedial cingulate, retrosplenial, and caudal parahippocampal cortices. The Journal of Comparative Neurology 438(3), 353-376.

Wu, L., Soder, R.B., Schoemaker, D., Carbonnell, F., Sziklas, V., Rowley, J., Mohades, S., Fonov, V., Bellec, P., Dagher, A., Shmuel, A., Jia, J., Gauthier, S., Rosa-Neto, P., 2014. Resting state executive control network adaptations in amnestic mild cognitive impairment. Journal of Alzheimer's Disease: JAD 40(4), 993-1004.

Zhao, Z.L., Fan, F.M., Lu, J., Li, H.J., Jia, L.F., Han, Y., Li, K.C., 2014. Changes of gray matter volume and amplitude of low-frequency oscillations in amnestic MCI: An integrative multi-modal MRI study. Acta Radiologica. pii: 0284185114533329. [Epub ahead of print]

Zijdenbos, A., Forghani, R., Evans, A., 1998. Automatic quantification of MS lesions in 3D MRI brain data sets: Validation of INSECT. Medical Image Computing and Computer-Assisted Interventation—MICCAI' 98. Springer Verlag Berlin, Heidelberg. pp. 439-448.

8.1. TABLES AND FIGURES

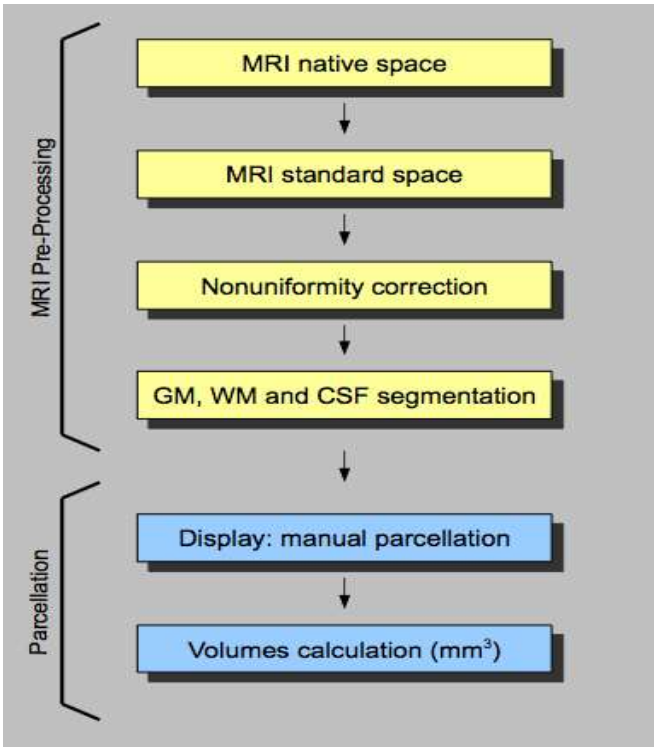

Figure 1: MRI analytic pipeline.

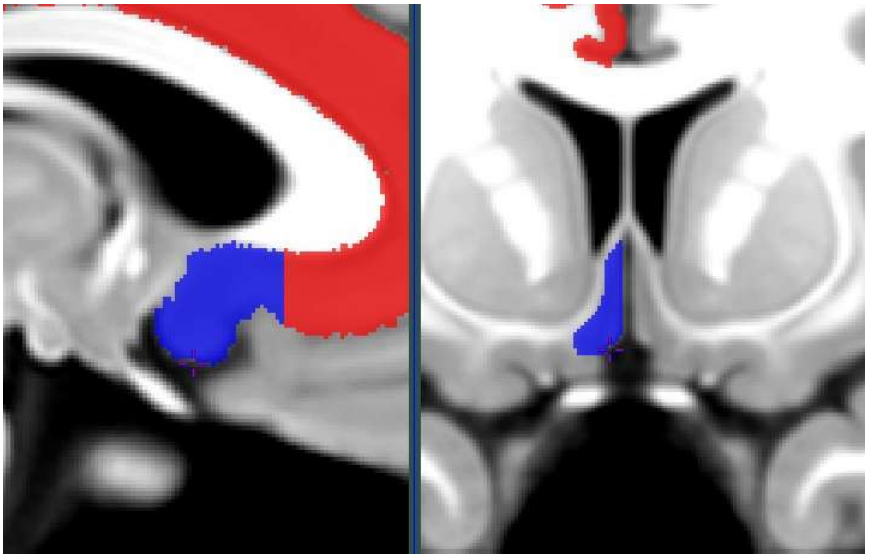

Figure 2: The SGC displayed in blue. Atlas by Fonov *et al*., 2009.

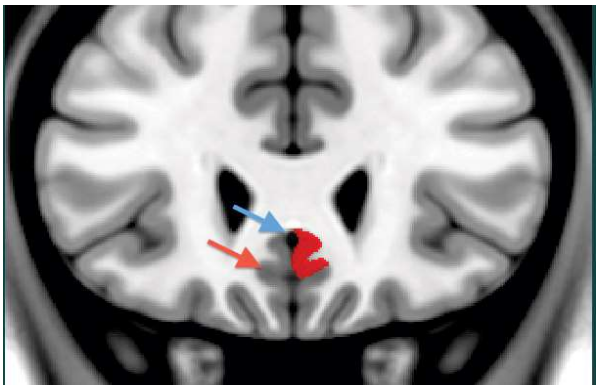

Figure 3: sACC in red. Blue arrow shows the cas and red arrow the cgs. Atlas by Fonov *et al*., 2009.

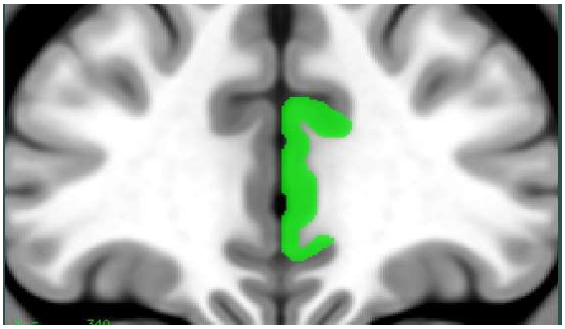

Figure 4: rACC in green. Atlas by Fonov *et al*., 2009.

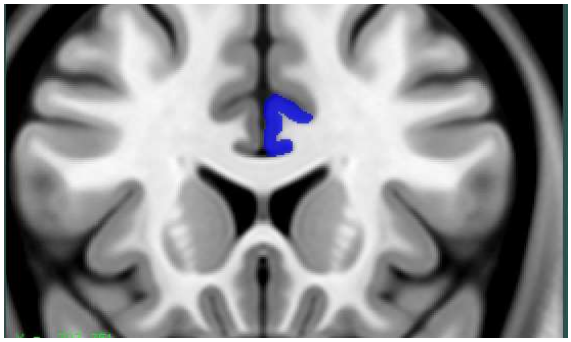

Figure 5: dACC in blue. Atlas by Fonov *et al*., 2009.

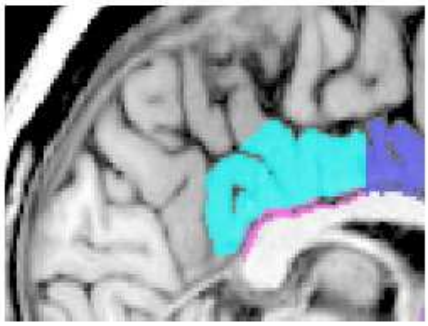

Figure 6: PCC in turquoise and RSC in pink, right below. From our sample.

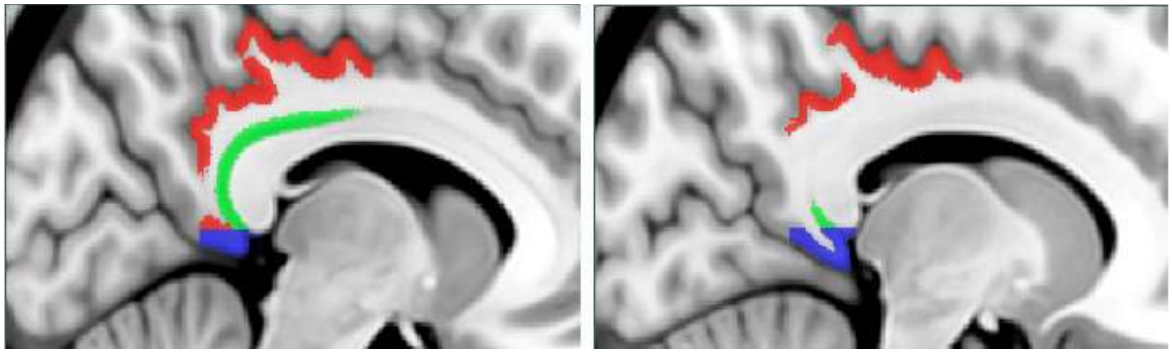

Figure 7: CMR in blue, PCC in red and RSC in green. Atlas by Fonov *et al*., 2009.

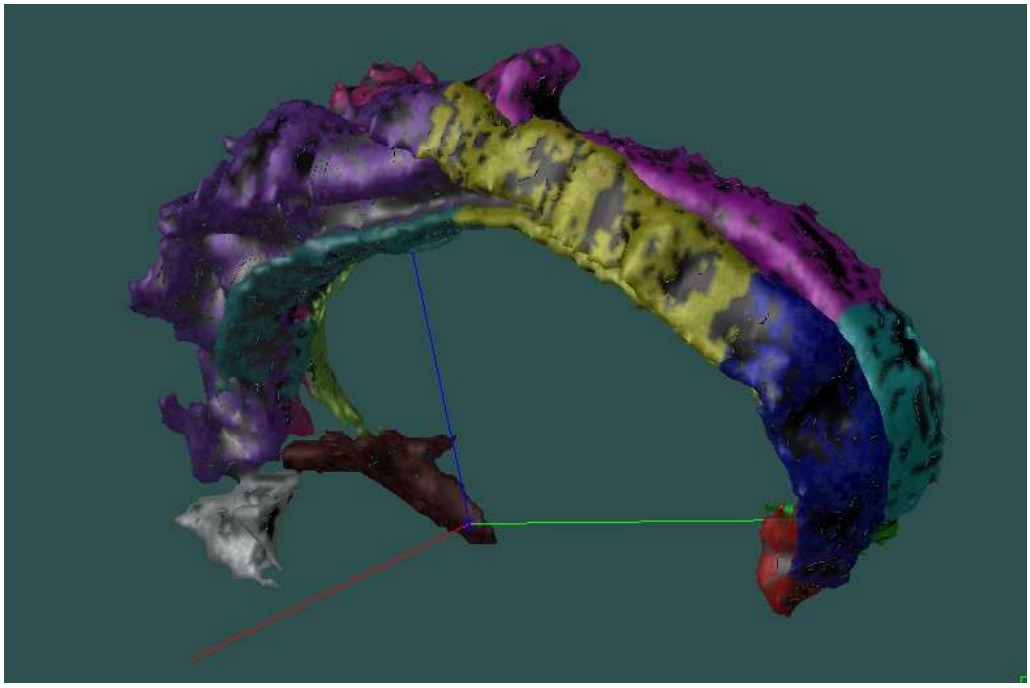

Figure 8: A 3D view of a cingulate gyrus manually parcellated. Different colors represent different subregions. The red line represents the X axis, the blue line represents the Z axis and the green the Y axis. The polygons were smoothed.

Table 1: Pooled mean volumes for each cingulate subregion.

Cingulate Cortex Subregions	Mean Volumes (SD)	
	Left	Right
SGC	583.88 (252.22)	556.33 (158.50)
sACC	620.25 (165.30)	696.17 (270.08)
rACC	2413.50 (771.54)	2191.67 (1259.87)
dACC	4559.75 (1050.76)	4005.42 (1327.18)
PCC	5138.17 (1063.21)	5223.58 (1218.65)
RSC	818.13 (265.39)	798.17 (247.98)
CMR	338.58 (168.67)	361.17 (160.66)
Total	14472.25 (2414.08)	13832.50 (3475.02)

SD = standard deviation; SGC = subgenual cortex; sACC = subcallosal anterior cingulate cortex; rACC = rostral anterior cingulate cortex; dACC = dorsal anterior cingulate cortex; PCC = posterior cingulate cortex; RSC = retrosplenial cortex; CMR = caudomedial region

Table 2: ICCs for the different cingulate subregions

Cingulate Cortex Subregions	ICC	
	Left	Right
SGC	0.53	0.56
sACC	0.78	0.94
rACC	0.93	0.99
dACC	0.98	0.99
PCC	0.94	0.83
RSC	0.36	0.38
CMR	0.41	0.33
Total	0.97	0.97

ICC = intraclass correlation coefficient; SGC = subgenual cortex; sACC = subcallosal anterior cingulate cortex; rACC = rostral anterior cingulate cortex; dACC = dorsal anterior cingulate cortex; PCC = posterior cingulate cortex; RSC = retrosplenial cortex; CMR = caudomedial region

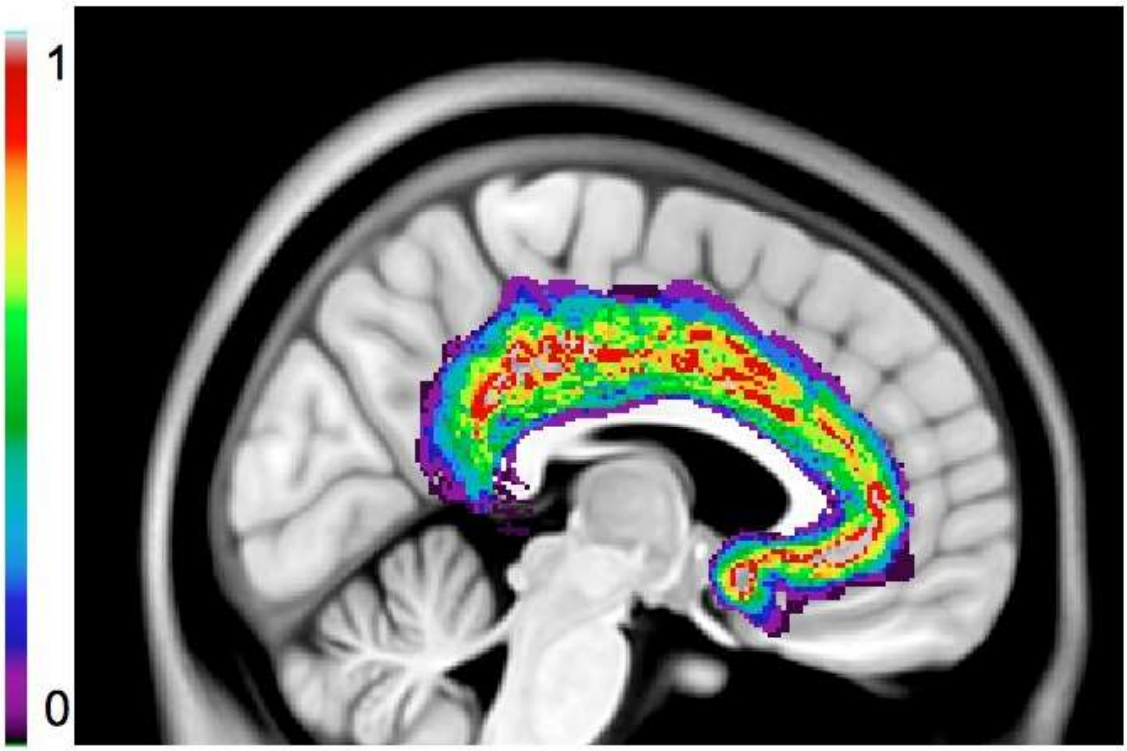

Figure 9: Probabilistic maps of binarized images of the parcellated cingulate gyri. Regions closer to 1 in the color palette represent the higher level of concordance between raters.

9. CONCLUSÃO

O objetivo do presente estudo foi o de introduzir um novo método para o parcelamento manual de todo o córtex cingulado, com um equilíbrio mais satisfatório entre confiabilidade inter-avaliadores e correlatos histológicos entre as sub-regiões. Como um todo, a análise de confiabilidade revelou um bom ICC, embora as áreas menores ainda precisem ser melhoradas. A modificação de pontos de referência para estas áreas deve ser considerada a fim de otimizar sua confiabilidade, mas o presente protocolo pode ser facilmente utilizado para as regiões mais amplas ou para todo o córtex cingulado. O novo marcador da divisão do córtex cingulado em anterior e posterior (Y = -10) é de fácil aplicação e situa-se aproximadamente no fim da área motora do cingulado, tornando assim a sua utilização recomendada.

10. ANEXOS

10.1. APROVAÇÃO DO CEP DA UFCSPA

10.2. APROVAÇÃO DO CEP DA MCGILL (ESTUDO ONDE FORAM REALIZADAS AS IRMs)

10.3. TERMO DE CONSENTIMENTO

10.4. GUIDE ON DISPLAY

10.5. CINGULATE GYRUS MANUAL PARCELLATION PROTOCOL (VERSÃO FINAL)

10.6. PSYCHIATRY RESEARCH: NEUROIMAGING, GUIDE FOR AUTHORS

UFCSPA

COMISSÃO CIENTÍFICA E COMISSÃO DE PESQUISA E ÉTICA EM SAÚDE

COMITÊ DE ÉTICA EM PESQUISA - CEP
UFCSPA

O Comitê de Ética em Pesquisa da UFCSPA, registrado na Comissão Nacional de Ética em Pesquisa (CONEP) sob o nº 075/05 em 23/07/04, analisou o Projeto:

Projeto: 12-990 **Versão do Projeto:** **Versão do TCLE:**

Pesquisadores:
YGOR ARZENO FERRÃO
THIAGO CASARIN HARTMANN

Título: CÓRTEX CINGULADO E SUAS SUBDIVISÕES: PROTOCOLO DE SEGMENTAÇÃO MANUAL EM RESSONÂNCIA MAGNÉTICA.

Esse projeto foi aprovado em seus aspectos éticos e metodológicos conforme as Resoluções 196/09 e demais Resoluções complementares. Toda e qualquer alteração do projeto, assim como eventos adversos graves, deverão ser comunicados a este CEP. Os TCLE, quando necessários, somente poderão ser utilizados após prévia e explícita aprovação (carimbo) de sua redação por este CEP".

Porto Alegre, 28 de maio de 2012.

Júlia S. Pereira Lima
Vice-Coordenadora CEP/UFCSPA

McGill

Faculty of Medicine
3655 Promenade Sir William Osler
Montreal, QC H3G 1Y6

Faculté de médecine
3655, Promenade Sir William Osler
Montréal, QC, H3G 1Y6

Fax/Télécopieur: (514) 398-3595

08 December 2009.

Dr. Pedro Rosa-Neto
McGill Centre for Studies in Aging
6825 Boulevard LaSalle
Verdun QC H4H 1R3

RE: IRB Study Number A12-M107-08A
Glutamatergic abnormalities in patients with early AD

Dear Dr. Rosa-Neto,

On December 07, 2009, at a meeting of the Institutional Review Board, a full Board review and approval were provided for the following consent form for the above-referenced study:

- Revised Consent Form for Participation as Control Subject in Research Protocol, English and French versions (IRB dated November 2009).

The investigator is responsible for ensuring that all documents approval by this IRB are reported to and meet the standards in effect at institutions where subject recruitment occurs and/or where study data is collected and retained. The Investigator must contact the individual Research Ethics Offices to fulfil this obligation. A failure to comply with this requirement may result in the invalidation of the study's data and a freezing of research funds.

Regards,

Roberta Palmour

Roberta Palmour, PhD
Co-Chair
Institutional Review Board

Cc: DH/REB
A12-M107-08A

CONSENT FORM FOR PARTICIPATION AS CONTROL SUBJECT IN RESEARCH PROTOCOL (Douglas Research Institute / Montreal Neurological Institute)

Project title: Glutamatergic abnormalities in patients with early Alzheimer's disease.

Principal Investigator:
Pedro Rosa Neto, MD, PhD (Douglas Research Institute; McGill Centre for studies in Aging)

Reason for the study

"Positron Emission Tomography (PET) is a nuclear medicine examination useful for the diagnosis of dementia. The standard radiopharmaceutical utilized in the clinical PET scans is [radioactive]FDG. PET [radioactive]FDG scans provide an index of brain energy consumption. In this study we will compare a novel radiopharmaceutical called [radioactive]ABP688 with [radioactive]FDG. PET [radioactive]ABP688 measures a brain protein called (glutamate type 5 receptor). Since "glutamate type 5 receptor" is involved in cell-to-cell communication, we believe that the novel radiopharmaceutical provides better information about the neurobiology of dementia compared to [radioactive]FDG." You are invited to participate because you have no neurological diseases and thus will be part of a healthy control group for the analysis of the data from patients with Alzheimer's disease.

Procedures:

Your participation in this study will involve three sessions of about one to two hours each. The first session consist of a clinical interview, a neurological examination and a series of computerized tests. The second session involves a Magnetic Resonance Imaging (MRI) study. The third session will involve a Positron Emission Tomography (PET) study with [radioactive]ABP688 (one hour) and a PET [radioactive]FDG study (one hour). The whole study will be conducted in a one-week time frame.

1) The memory test session aims a detailed appraisal of the cognitive functioning and will consists in the administration of the following battery of cognitive tests:

Verbal and nonverbal list learning tests
Selected subtests from the WASI (Weshler Abbreviated Scale of Intelligence)
Colour-word interference test (Stroop)
Verbal and nonverbal span tests
Boston naming test
Token test
Test of fluency
Tour of London
Complex figure test

The certified clinical neuropsychologist Dr. Vivian Szicklas and her assistant will be involved in the administration and interpretation of these tests. The cognitive battery will be administrated in two distinct sessions of 1.5 hour each for a total of 3 hours. According to your needs, we will provided breaks during the test sessions.

2) A saliva sample will be collected for genetic determination of the apolipoprotein E gene. The apolipoprotein E genetic information is required for [radioactive]FDG PETscan evaluation.

FORMULAIRE DE CONSENTEMENT POUR LA PARTICIPATION COMME PERSONNE EN BONNE SANTÉ DANS UN PROTOCOLE DE RECHERCHE
(Institut Recherche Douglas / Institut Neurologiques de Montréal)

Titre du projet : Anomalies du glutamate dans les patients avec maladie d'Alzheimer (MA) au tout début.

Principal Chercheur:
Pedro Rosa Neto, MD, PhD (Institut Recherche Douglas; Centre McGill d'études sur le vieillissement)

Raison de l'étude

La tomographie par émission de positons (TEP) est un test de médecine nucléaire utile pour l'évaluation des troubles cognitifs. La TEP conventionnelle implique l'injection de glucose radioactif pour une courte période (FDG). Cet examen donne une mesure du fonctionnement du cerveau, qui est anormale dans la MA. Dans cette étude nous allons comparer les résultats obtenus avec le FDG et un nouveau marqueur des récepteurs du récepteur glutamate type 5 (ABP688). Nous croyons que le ABP688 est plus sensible que le FDG pour le diagnostic précoce de la MA. Vous êtes invités à participer parce que vous n'avez aucune maladie neurologique et ferez ainsi partie d'un groupe de personnes en bonne santé pour l'analyse des résultats chez les patients avec la MA.

Procédures:

Cette étude comporte trois séances d'environ une ou deux heures chacune. La première séance consiste en une entrevue clinique, un examen neurologique et une épreuve de mémoire devant l'ordinateur. La deuxième séance consiste en une imagerie par résonance magnétique (IRM). La troisième séance impliquera en une TEP) avec [^{11}C]ABP688 (environ une heure) et une TEP [^{18}F]FDG (environ une heure). L'étude devrait être complétée dans une semaine.

1) La session de test de mémoire vise une évaluation détaillée du fonctionnement cognitif et consistera en l'administration de la batterie de tests cognitifs suivante:

- Tests d'apprentissage de liste verbale et non-verbale
- Sous-tests sélectionnés du WASI (Weshler Abbreviated Scale of Intelligence)
- Test d'inférence couleur-mot (Stroop)
- Tests d'empan verbaux et non-verbaux
- Test de dénomination Boston
- Test des jetons
- Test of fluidité verbale
- Tour de Londres
- Test de figure complexe

La neuropsychologue clinique certifiée Dr. Viviane Szicklas ainsi que son assistante seront responsables de l'administration et de l'interprétation de ces tests. La batterie cognitive sera administrée au cours de 2 sessions distinctes de 1.5 heures chaque, pour un total de 3 heures. Selon vos besoins, nous fournirons des pauses au cours des sessions.

2) Un échantillon de salive sera recueilli afin déterminer le type de gène de l'apolipoprotéine E que vous avez. Cette information génétique sera utile pour analyser les résultats des TEP.

Guide on Display

About

Basically, a guide on how to do CNS structures segmentation and volumetrics using MINC files. I used some info from these other guides: http://www.bic.mni.mcgill.ca/users/kate/Howto/Display.html http://wiki.bic.mni.mcgill.ca/index.php/DisplayManual

How to open MINC files?

You'll need the Display program (there are other programs to do that, but they're not the scope of this guide). First open a terminal (the command line prompt) and type Display 'name_of_the_file.minc'. For instance:

Display '/home/thiago/Desktop/mni_icbm152_nlin_sym_09b_minc2/mni_icbm152_t1_tal_nlin_sym_09b_hires.mnc'

There's a way to make things easier: after you typed Display (always capitol D and always space after 'Dysplay'), just drag the MINC file icon from your desktop to the terminal and it should appear as above.

Recommended placement of Display windows

- Terminal window: lower left corner
- Keyboard menu: lower right corner
- 3D object window: upper left corner (the one with the cross-hairs in the centre of the window)
- 4-panel window: top centre (window needs to be enlarged once files have been loaded)

Also, I recommend closing any unnecessary windows and minimizing all other applications so that the 4-panel window can be viewed with no other layers above or below it. When using the “Save Slice Image” option, it seems that everything in the panel (including bits from other windows) of interest gets saved.

Adjust an image's colour coding

On the keyboard menu, pop to main menu [space], select Colour Coding [D], select desired colour scheme:

- Grey Scale [D]
- Spectral [S]
- Red [E]

- Green [R]
- Blue [T]
- HotMetal [F]

Apparently, the Colour Coding [D] menu serves only for visualization preferences, so have fun choosing the best for you.

Also, you can manually change the colour scale by the bar on the left of the 4 panel window. Just move the green and blue little bars across it and thy will shall be done. Or you can type the range you want by selecting Range [H] on the Colour Coding [D] menu.

You can adjust the colour over and under the two little bars on the colour scale bar. Like this: in the Colour Coding Menu, select Overcolour [X] and type “transparent”, or any other colour, at the prompt in the terminal window. Then, select Undercolour [Z] and type “transparent”, or any other colour, at the prompt in the terminal window.

Basic 4 panel commands

Well then, you already chose the best colour scheme, now it's time to learn some basic navigation tips on the 4 panel window.

Firstly, a brief explanation of what it is. You can see three brain images on that: in a 3D Cartesian coordinate system, the upper left represents the sagital X-axis (latero-lateral), the upper right represents the coronal Y-axis (rostro-caudal) and the lower left represents the axial Z-axis (ventro-dorsal). The lower right empty panel will serve for generation of a three dimensional slice (we'll see how to do that below).

The basic commands:

- To navigate in each axis you can use the left mouse button to drag the cross-hair along them.
- To change the slice, move the mouse cursor to the axis of interest and press 'minus' [-] or 'plus' [+] signs on the keyboard, or press and drag the middle mouse button.
- To segment some structure, press and drag the right mouse button on the axis and the slice of interest.

Now here's an interesting thing: if you press 'SHIFT' on your keyboard, the mouse button command will change. The same thing will happen if you turn on the 'CAPS LOCK':

- You can move the whole slice picture by pressing 'SHIFT' + left mouse button.
- You can zoom in or out by pressing 'SHIFT' + middle mouse button.
- You can erase previous segmentation by pressing 'SHIFT' + right mouse button.

You can stretch or enlarge the desired axis by dragging the window center (where the two blue lines cross each other) with the left mouse button.

Note: when using Mac OS, the zoom works by pressing 'command' and 'SHIFT' with the middle mouse button.

Segmenting menu

On the Segmenting [F] menu, you can configure the Segmenting parameters. I'll describe here the

commonest features:

- To set the brush radius, select XY Radius [F] and type the new radius on the terminal window. The minimum accepted is 0.1, which is the size of a voxel.
- You can choose the colour you're painting by selecting Set Paint Lbl [D]. Each colour has a number, you must type its correspondent number in the terminal window. Zero is no colour at all. The colour designates the label you're working on. You can label multiple areas and correlate them thereafter (I guess).
- You can set also the eraser colour by selecting Set Erase Lbl [1]. The colour numbers are the same for painting. Sometimes when you're configuring other things, the program will ask you to reconfigure the eraser (don't ask me why), always keep it on zero.
- In order to fill a drawn circumference, select Label Fill [E]. You must put the cross-hair inside the circumscribed area you want to fill and then press the [E] button on your keyboard.
- To fill the whole slice you're working on, select Label Slice [A]. It only works if you keep the mouse cursor on the slice of interest and press the [A] button.
- To clear the whole slice, the command is Clear Slice [S]. You must do the same as above, and press [B] to confirm it.
- To clear only one label, the command is Clear Fill [T].
- Press [V] to calculate the volume of the painted area. It'll calculate the volume of all painted areas of the same colour, in all slices and axes you've painted it. To change the volume to be calculated, simply change the colour on the [D] option (Set Paint Lbl).
- If you segment something wrong, just hit the Undo [7] button.

How to create a 3D rendering of a segmented area?

Click somewhere on the part of the label (label = colour) that you want to render in 3D. Go to the “Create Surface” menu (G). Select “Label Bin-Isosurface” (G). Then, in the terminal, type the min and max of the label - for example, if your value is 1, type 0.5 1.5. This should do a marching cubes rendering of the label in the objects window.

To erase the 3D rendering, the command is Reset Surface [X], inside the Create Surface [G] menu.

How to save your work?

Go to the File [T] menu.

Saving the 3D rendering

Click in Save File [D], then choose a name for your 3D rendering. The program will automatically put the .obj extension and the file will stay on the directory with your username.

Saving the labels

You can save all the labels you've segmented by clicking the Save Labels .tag [R] button or only the current label by clicking Save Curr Lbl .tag [T] button. The program will do the same as above, but the extension will be .tag.

How to load files?

You can do it by the File [T] menu once you've opened the MINC file you were working on. You can load either the 3D rendering or the labels by clicking the correspondent buttons ([E] for labels and [F] for the 3D). You need to type on the terminal the file name *and* the extension name.

You can load the desired 3D rendering file directly from the terminal window as well. In order to do that, just put the name of the saved 3D rendering right after the MINC file name, as below:

Display '/home/thiago/Desktop/mni_icbm152_nlin_sym_09b_minc2/mni_icbm152_t1_tal_nlin_sym_09b_hires.mnc' filename.obj

To load the label(s) from the terminal, you need to type '-label' on the terminal window, between the MINC file name and the saved label(s) file name, as below:

Display '/home/thiago/Desktop/mni_icbm152_nlin_sym_09b_minc2/mni_icbm152_t1_tal_nlin_sym_09b_hires.mnc' -label filename.tag

You can load both the 3D rendering and the label(s), like this:

Display '/home/thiago/Desktop/mni_icbm152_nlin_sym_09b_minc2/mni_icbm152_t1_tal_nlin_sym_09b_hires.mnc' filename.obj -label filename.tag

Partial Automatic Segmentation

- You can paint only gray matter as long as you have the chosen MRI mask. A mask is a file you can load into Display with automatic separation of gray matter, white matter and CSF. This guide does not purpose to teach how to do the mask, only how to load it into Display and how to use it to paint only gray matter.
- First you need to open the files you want, typing 'Display nameofthefile.mnc nameofthemask.mnc'. By doing this, you will be opening the two files required.
- Now you need to set the upper and lower colours as 'transparent'. Go to Colour Coding menu [D] and choose first Under Col [Z]. The program will ask which colour components you want: go to the terminal window and type '0 0 0 0'. Then choose Over Col [X], inside the Colour Coding menu [D], and do the same.
- Now, go to Range [H], still inside the Colour Coding menu [D]. Type '3 3' on the terminal window.
- Next step is the Slice View menu [S], where you will hit Curr Volume [T] and set it to '1'.
- Go back to the Colour Coding menu [D], where you can adjust the colour of your choice and

regulate the image on the colour bar (see the Display guide above for detailed explanation on this).

- The final step is setting the threshold to segment only gray matter. Go to Segmenting menu [F] and hit Set Threshold [Y]. Type '1.5 2.5' on the terminal window: that's the limits for segmenting only gray matter. Now you will be able to segment only gray matter.

Observations and hints

- In threshold segmentation I personally prefer not to set the planes before I start (the planes model for cingulate segmentation is discussed further). I would rather set them as the segmentation goes along.
- Although a very good tool, the masks are not entirely accurate, so trust in your judgment when making decisions about including areas as gray matter.
- You don't need to segment slice per slice in a straight way, the most important thing to do is to identify the anatomic structures.
- Sometimes a sulcus will gradually disappear as you progress (ex.: the paracingulate sulcus ventral part). If that happens, keep segmenting the part where the sulcus should be, in the previous sulcus same orientation.
- A sulcus may have a wide fundus instead of a thin one. In this case, the line in between both banks is traced in the fundus middle.
- When tracing lines on sagittal slices to unite separate parts of the same sulcus, trace them on several slices. Try to follow the sulci orientation on all sagittal slices, even though the lines seem to change their position on subsequent slices (i.e. the line goes rostrally on the next slice, for example). Also, it doesn't matter if the line isn't perfectly straight on the same slice, as long as it connects both sulcus parts by the shortest path.

Cingulate Gyrus Segmentation

Step 1: Sulci patterns identification.

In this step, the purpose is to identify the most relevant sulci used as landmarks for the cingulate gyrus segmentation. We will try to cover the most important pattern variations, according to previous literature. The rules to segment each pattern are discussed further. It is easier to perform this identification through the sagittal slices.

Cingulate sulcus (cgs): In our guideline, for reliability purposes, we consider it as always beginning as the continuation of marginal ramus (mr), rostrally, and following the corpus callosum (cc) orientation. It is also the deepest corpus callosum oriented sulcus, with depth defined as the distance of the sulcus fundus from X = 0 mm (the midline), i. e. the last sagittal slice where you can see cerebrospinal fluid (CSF) inside the sulcus. The depth can also be checked on coronal and axial slices.

Variability: Basically, there are four main patterns, according to the picture below:

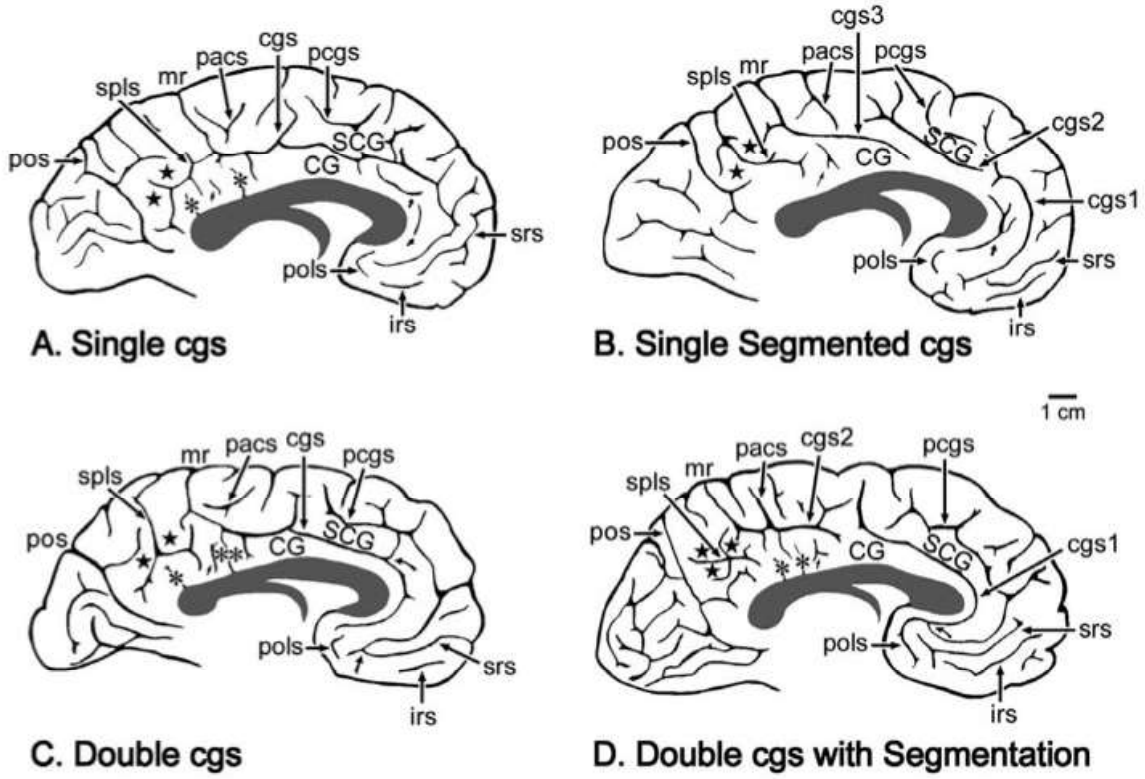

Figure 1: Four patterns of the cingulate sulcus and its correlates variation. CG, cingulate gyrus; SCG, superior cingulate gyrus (paracingulate gyrus); pols, paraolfactory sulcus (anterior subcallosal sulcus); irs, inferior rostral sulcus; srs, superior rostral sulcus; cgs, cingulate sulcus; pcgs, paracingulate sulcus; pacs, paracentral sulcus; mr, marginal ramus; spls, splenial sulcus (subparietal sulcus or suprasplenial sulcus); pos, parietooccipital sulcus. Taken from Vogt et al. (2004).

Paracingulate sulcus (pcgs): Every sulcus running in parallel with the cgs on the medial surface, externally, is named paracingulate sulcus (Paus et al. 1996). It is not always present and it can have interruptions, as seen above (fig 1).

Intralimbic sulci (inls): When there are sulci running in parallel with the cgs internally, i. e. between the corpus callosum and the cgs, these are the intralimbic sulci (Paus et al. 1996).

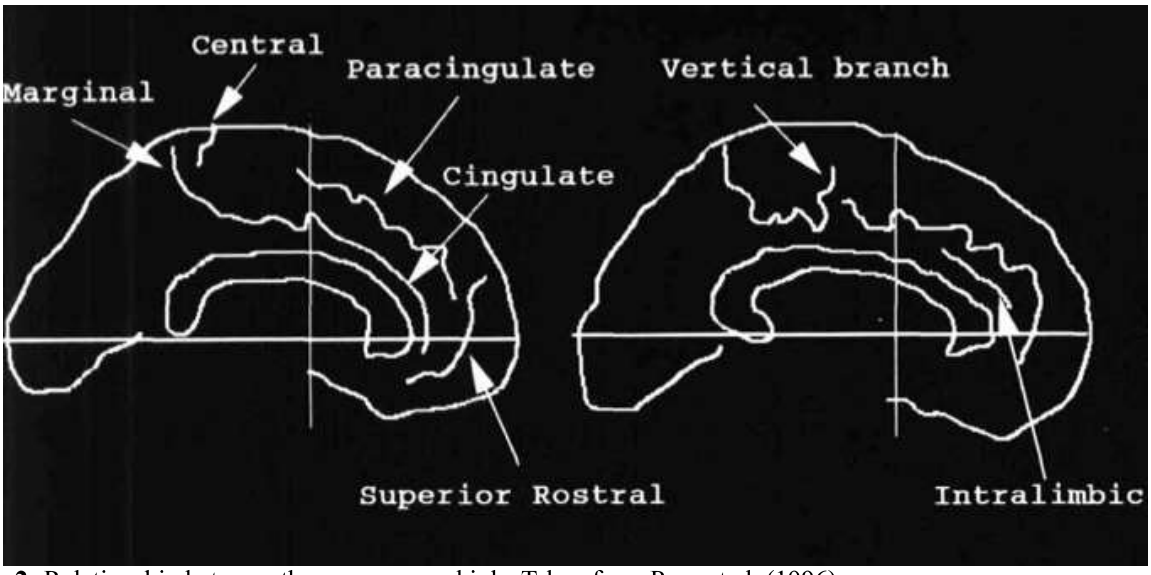

Figure 2: Relationship between the cgs, pcgs and inls. Taken from Paus et al. (1996).

Callosal sulcus (cas): It is the sulcus between the cc and the cingulate cortex. It follows the cc orientation.

Superior rostral sulcus (srs): it is defined as the nearest sulcus above the AC–PC axis on the anterior portion of the medial surface (Crespo-Facorro et al., 1999).

Cingulate sulcus end: The beginning of the cgs in our guideline is the mr. Therefore, the end is considered the other extreme. The cgs may end in three different patterns (adapted from Ono et al. 1990):

(1) turning ventrally below the cc genu,
(2) connecting with the srs or
(3) ending before it turns ventrally or connects with the srs.

Splenial sulcus (spls): The spls (also subparietal sulcus or suprasplenial sulcus) is defined as the first sulcus parallel with cas, after the marginal ramus appearance. It usually has an “H” form (fig 3), but it is very irregular among the subjects, with many interruptions.

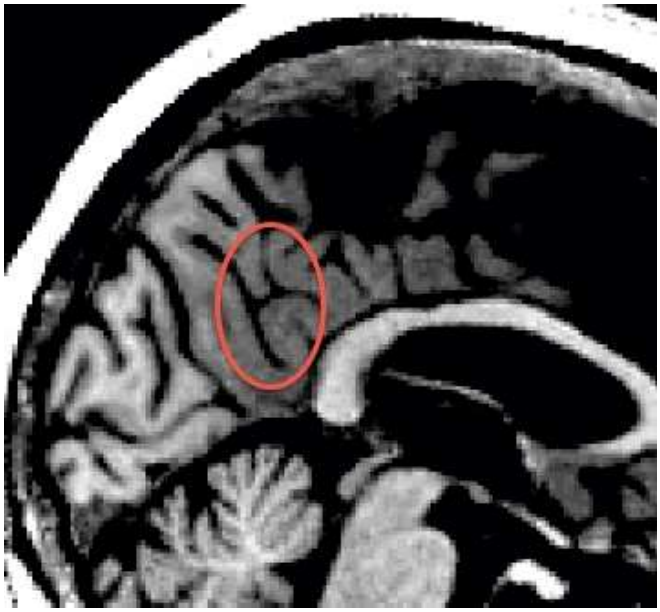
Figure 3: The red circle highlights the spls. Taken from our sample.

Marginal ramus and splenial sulcus relationship: It may present with four patterns (Ono et al. 1990):

(1) with connection to the splenial sulcus,
(2) with a side branch not connected with the splenial sulcus,
(3) with a side branch and connection with the splenial sulcus and
(4) without both.

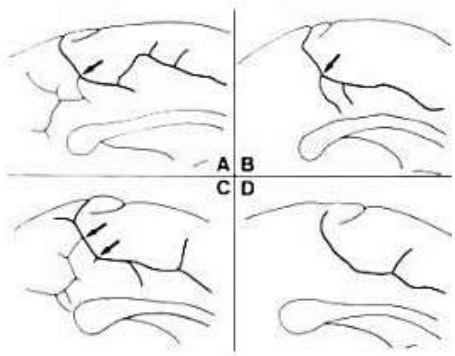

Figure 4: Four patterns of the mr and spls relationship. Each letter represents an example from above, respectively (A=1, B=2, etc.). Taken from Ono et al. (1990).

Anterior calcarine sulcus (acals): The acals is the junction of the calcarine sulcus and the parieto-occipital sulcus (Fig 5), also called calcarine and parieto-occipital fissures. Both are mostly proeminent in practically all regular brains, with incidence rates of 92% for the calcarine sulcus and 100% for the parieto-occipital sulcus (Ono et al. 1990).

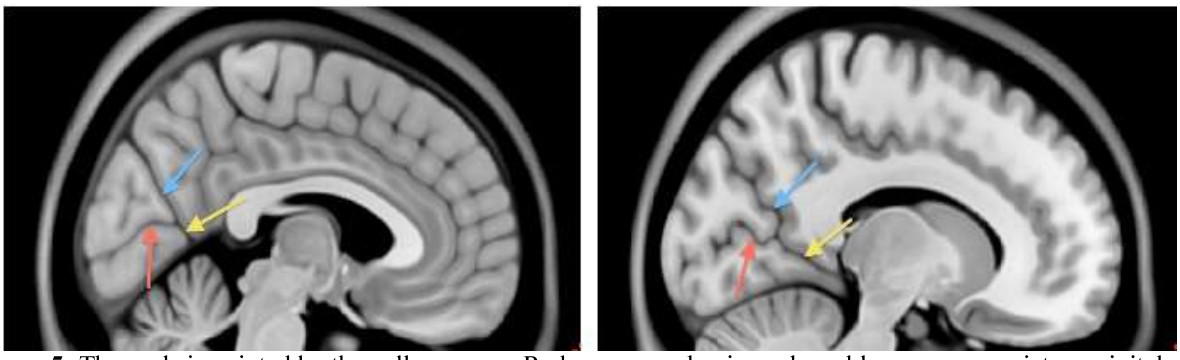

Figure 5: The acals is pointed by the yellow arrow. Red arrow = calcarine sulcus; blue arrow = parieto-occipital sulcus. The right picture is a more lateral view from the same brain atlas. Taken from an atlas by Fonov et al. (2009).

Posterior subcallosal sulcus (pscs): It is the sulcus that depicts the posterior end of the frontal lobe medial surface (Fig 6) (Richardson et al. 2009).

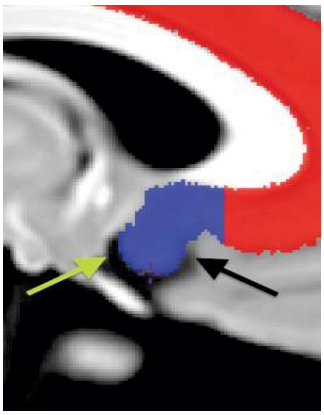

Figure 6: Ascs and pscs. Black arrow shows the ascs, green arrow shows the pscs. Both sulci tend to merge ventrally (see the cross cursor). Taken from an atlas by Fonov et al. (2009).

Anterior subcallosal sulcus (ascs): The ascs is the first anterior sulcus parallel to the pscs. It is also called anterior para-olfactory sulcus. Spasojevic et al. (2011) found the ascs in 86,9% of their 84 brain hemispheres sample. It is a small sulcus, usually with vertical orientation, and perpendicular to the cc (Fig 6). It was previously classified into four different types (Spasojevic et al. 2011):

(1) ascs in form of vertical or slightly oblique line,
(2) ascs in form of letter C or inverted letter C,
(3) ascs in form of letter S or inverted letter S and
(4) ascs not classified in any of previous types.

Step 2: Cingulate subdivisions and its borders.

Here, the objective is to identify all the cingulate subdivisions prior to the manual segmentation. We adapted the planes model from McCormick et al. (2006). The main modification here is the last plane, which defines the posterior boundary of the anterior cingulate cortex (ACC). This was done because the sulci near to marginal ramus present great variability in our sample, making it less reproducible. The other ones are properly located, as they proved to be worthy, since more recent papers found important differences among them (Ichikawa et. al. 2011, Gunning et. al. 2009, Lindberg et. al. 2009).

The first plane is plane A: it is set on the coronal plane, one slice forward from the slice in which the two sides of the anterior corpus callosum are no longer connected through the genu. The next plane is B, one coronal slice before the putamen is seen within the basal ganglia. Plane C is set on Y = -10 mm (i.e. a vertical line on the sagittal plane, 10 mm caudal to the anterior commissure plane). That landmark suits well with the end of the caudal cingulate motor area (Paus et al. 1996). Also, it sets the end of the gigantopyramidal field of Braak (Braak H., 1976). Plane B is the only plane that can be set differently among cerebral hemispheres. Figure 7 shows the ACC subdivisions. The same nomenclature is used in this protocol, except for the subgenual ACC, which is named subgenual cortex (SGC) to facilitate abbreviations.

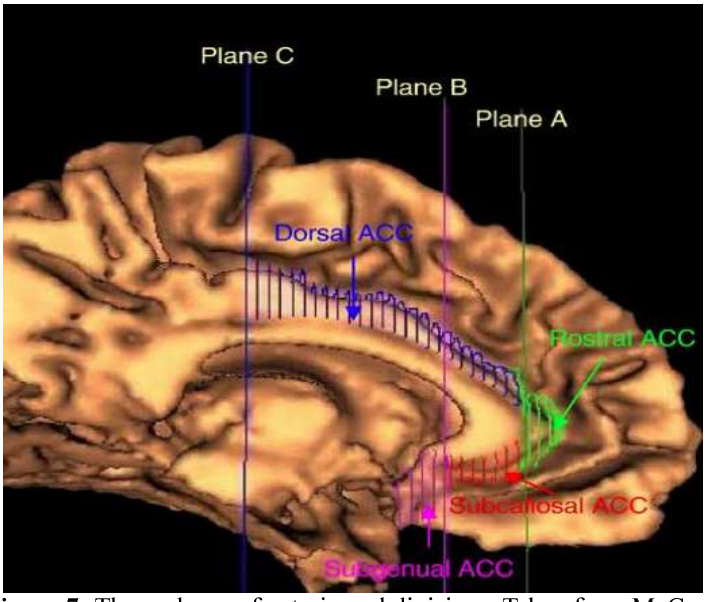

Figure 7: Three planes of anterior subdivisions. Taken from McCormick et al. 2006.

The posterior areas are the posterior cingulate cortex (PCC), the retrosplenial cortex (RSC) and the caudomedial region (CMR). PCC is the continuation of dorsal ACC (dACC), except for the area surronding cas, namely the RSC. CMR is a region comprising parts of the PCC, the RSC and the parahippocampal cortex (Vogt et al. 2001). It is delineated following the PCC and the RSC, ventral to the cc splenium (Fig 8).

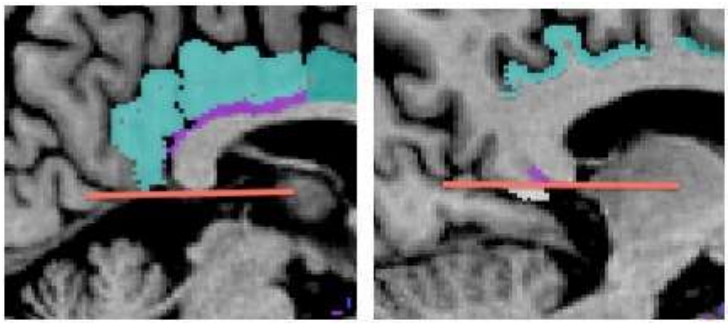

Figure 8: The border between PCC + RSC and the CMR is indicated by the red line. The first picture is from a more medial view of the same hemisphere portrayed in the second one. PCC is colored in light green, dACC is in dark green, RSC in purple and CMR in white. Taken from our sample.

Step 3: General segmentation rules.

There are some general rules that apply in this entire protocol. Here they are displayed in topics, in order to favor understanding. Exceptions to these rules may rise in any given cingulate subdivision. They will be discussed in further steps, as they appear.

- There is a variability that must be taken into account and may occur frequently: the interrupted sulci. In this case, one must always try to unite both parts by the shortest possible path drawn in several sagittal slices.
- Sometimes a sulcus change will be needed. When it happens, three rules are applied in the following order: the transition have to be smooth through manifold axial or coronal slices. In addition, the line connecting a primary sulcus to a secondary must follow the orientation of the first one in sagittal slices. The change also must be performed through the shortest possible path between both sulci.
- Every time a sulcus change must be performed, there is one thing that must be remembered: the cingulate cortex always tend to follow the cc orientation.
- This guide will refer to the terms shown in figure 9.

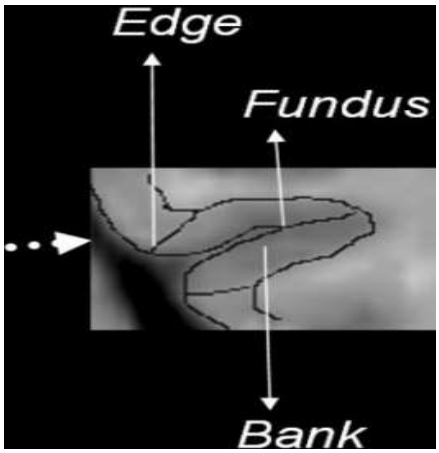

Figure 9: The parts of a sulcus. Taken from Bonilha et al. 2004.

- The limits defined in between sulci banks must be traced with a line following the sulcus bottom direction. (Fig 10) This avoids you from taking adjacent cortices.

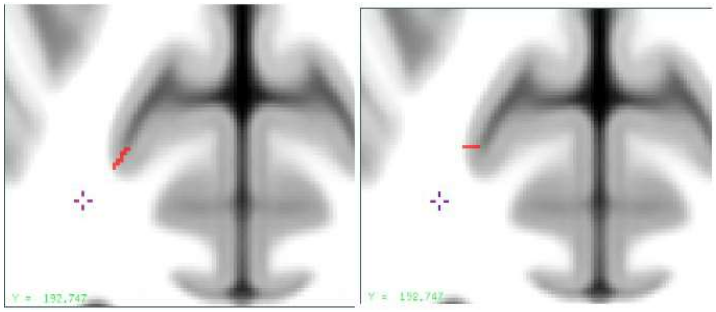

Figure 10: How to segment in between sulci banks. The left picture is correct, while the right one is not. Taken from an atlas by Fonov et al. (2009).

- Sometimes it is not possible to see CSF inside both banks of a given sulcus. In this case, the surrounding gray matter assumes the sulcus form, and therefore must be segmented right in the middle, where the CSF should be (Fig 11).

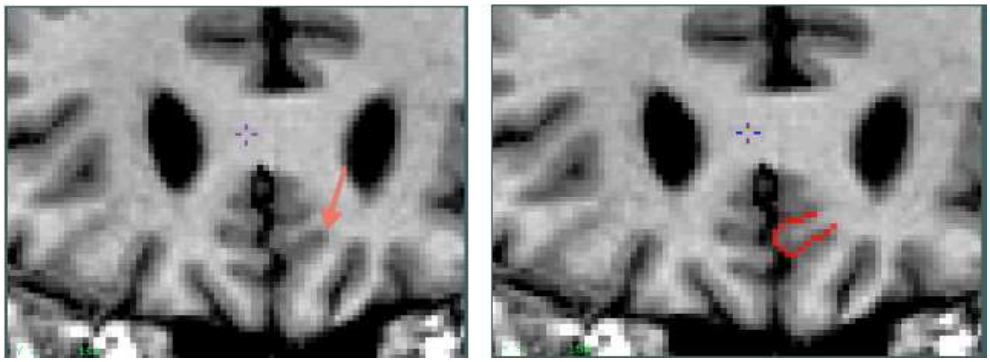

Figure 11: How to proceed when there is not possible to see CSF inside a sulcus. The red arrow points the sulcus to be segmented. The second picture shows an example of the same sulcus as it should be parcellated. Taken from our sample.

- In case of difficulty in any structure identification, use the other axes to help in its definition (Bonilha et al. 2004).
- The Display program allows partial automatic segmentation (see Guide on Display section). It means that it is possible to automatically separate CSF, gray matter and white matter prior to manual segmentation.

Step 4: The Anterior Cingulate Cortex (ACC).

The rules for ACC and its subdivisions parcellation are described here. See figure 6 to view the ACC subdivisions. The SGC will be discussed in another section.

The first area to be segmented will be the **subcallosal anterior cingulate cortex** (sACC). Take the most caudal coronal slice before the putamen appears to begin (plane B – Fig 12). That will be the ventral-posterior border of sACC. This corresponds well with the point of transition between the horizontally oriented subcallosal continuation of the cingulate gyrus and the beginning of the more vertical cytoarchitectural area of the paraterminal gyrus (McCormick et al. 2006). Start by identifying the callosal, cingulate and/or superior rostral sulci in the coronal slices, ventrally to corpus callosum. Set the cingulate cortex limits in the cingulate sulcus fundus (inferior), or superior rostral sulcus fundus (see below), and at the edge of the callosal sulcus dorsal bank (superior). Figure 13 shows an example of a coronal slice with a parcellated sACC.

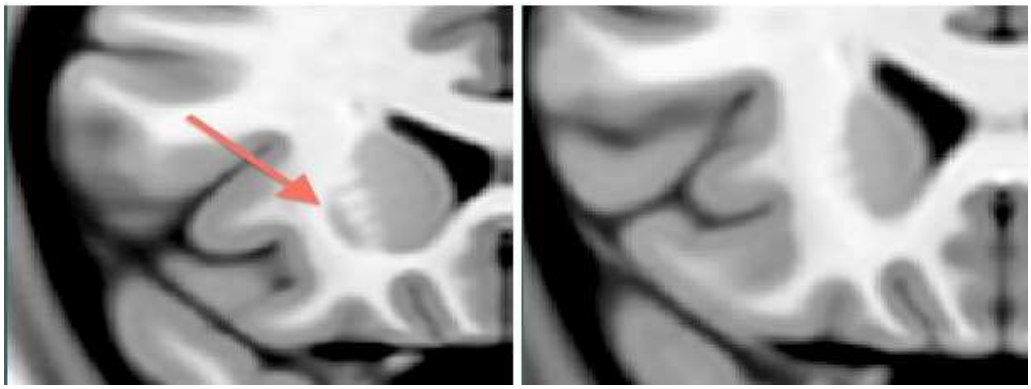

Figure 12: The right putamen in a coronal slice, marked by the red arrow. The right picture is from a more anterior coronal slice, it does not show the putamen anymore. Taken from an atlas by Fonov et al. (2009).

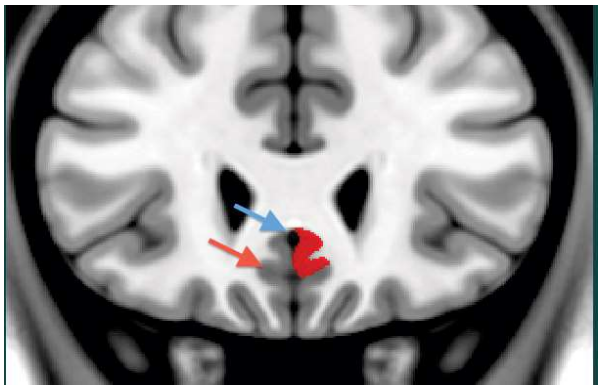

Figure 13: Left sACC parcellated in a coronal slice. The red arrow shows the cingulate sulcus fundus and the blue one shows the callosal sulcus dorsal bank edge, both in the right hemisphere. Note that it is possible to see both sulci above the cc as well. Taken from an atlas by Fonov et al. (2009).

If any doubt arises about which slice marks the putamen first appearance, try to segment it. Taking into account that the putamen corresponds to gray matter and the program only segments gray matter (see Guide on Display about how to configure it), the first slice showing it will be the first slice where you can segment it. However, this rule only applies here. The automatic segmentation is not entirely accurate, so thrust your judgment above it in most cases. This is particularly important in some areas described further.

Stop when you reach plane A. The next region is the **rostral anterior cingulate cortex** (rACC). Go segmenting the fundus of the ventral and dorsal cingulate sulci (above and below the cc, in the coronal view). Eventually, a switch to the axial slices is needed, because it is easier to visualize the cingulate sulcus rostral part. The plane A defining slice is also parcellated as a part of the rACC.

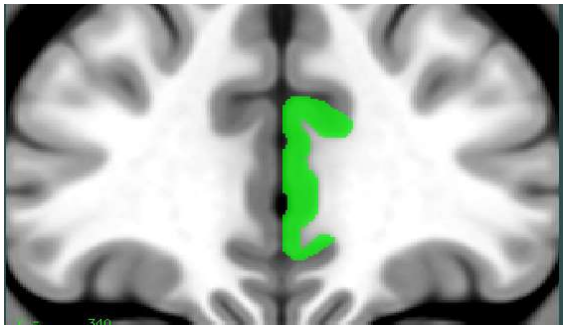

Figure 14: Left rACC parcellated in a coronal slice. Taken from an atlas by Fonov et al. (2009).

The region caudal to plane A until plane C, dorsally to corpus callosum, is the **dorsal anterior cingulate cortex** (dACC). The cortical area between the callosal sulcus ventral bank edge

and the cingulate sulcus fundus is segmented.

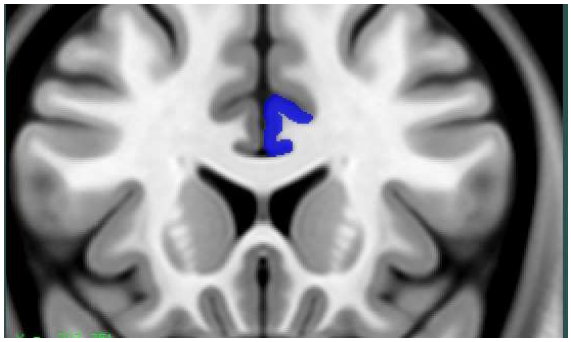

Figure 15: Left dACC parcellated in a coronal slice. Taken from an atlas by Fonov et al. (2009).

Variability specific rules:

Sometimes there are parallel sulci running with the cingulate sulcus (inls and pcgs – see Step 1). When these secondary sulci become the deepest and stay this way until the end, throughout the dorsal, rostral and/or subcallosal parts of cingulate cortex, they become the cingulate sulcus continuation and therefore should be segmented like that. However, the paracingulate or intralimbic sulci will only be segmented as the cingulate sulcus if they become undoubtedly the deepest or if the marginal ramus connected sulcus ends before it arches around the corpus callosum genu. Preference will always be given to the marginal ramus connected sulcus, especially if it follows the whole corpus callosum extension, arching around its genu. When appropriate, the sulcus change must be performed around the point where the secondary sulcus starts to be deeper than the primary one.

The cingulate sulcus may end in three different ways (see Step 1). In both last cases, the cingulate cortex inferior boundary becomes the srs. In the third case, a straight line following the cingulate sulcus direction must be drawn on sagittal slices uniting the cgs with the srs.

See Step 3 for general rules that may apply in these cases.

Step 6: The Posterior Cingulate Cortex (PCC) and Retrosplenial Cortex (RSC).

The PCC segmentation follows the dACC orientation, starting at the plane C coronal slice. However, the PCC ventral limit will be the cas dorsal bank edge instead of its ventral bank, because the cortex surrounding the cas is the RSC (Jones et al. 2006). Figure 16 illustrates it.

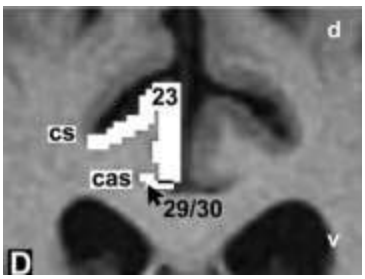

Figure 16: The PCC/RSC relationship. Cs = cgs. The numbers represent Brodmann areas. Taken from Jones et al. 2006.

Variability specific rules:

Even though Jones et al. (2006) preferred to avoid segmenting Brodmann area 31 (which surrounds the spls), they also stated that it is difficult to set its limits in a macroscopical level. For reliability purposes, the PCC dorsal limit was defined in this protocol as the spls fundus. It often gives birth to vertical branches towards cc, which are included as part of PCC. This sulcus is very irregular among subjects (see Step 1), so when it interrupts itself, a line must be drawn in the sagittal plane, connecting its edges by the shortest path possible. These lines must always connect its cc parallel parts, even when the vertical branches towards the cc form the shortest path (Fig 17).

In summary, two main rules are kept in mind when segmenting the PCC: the parcellation should follow the cc orientation, and, in case of any doubt in defining its posterior limits, one must try to segment always closer to the cc.

The mr may present with four patterns – see Step 1 (Ono et al. 1990):

(1) with connection to the spls,

(2) with a side branch not connected with the spls,

(3) with a side branch and connection with the spls and

(4) without both.

The first three ones rule is to segment the first branch parallel with the cas and connected to the mr as the spls, connecting it with a straight line on sagittal slices to the actual spls. Caution is needed because sometimes this side branch is very small. It should always work as a cgs continuation. As for the fourth pattern, the rule is to draw a straight line also on sagittal slices from the spls horizontal part to the cgs end, following the spls horizontal part direction (Fig 18). When the spls ends before the cc end, a line must be drawn straight down on a medial sagittal slice, connecting the spls end with the hemisphere end (Fig 19).

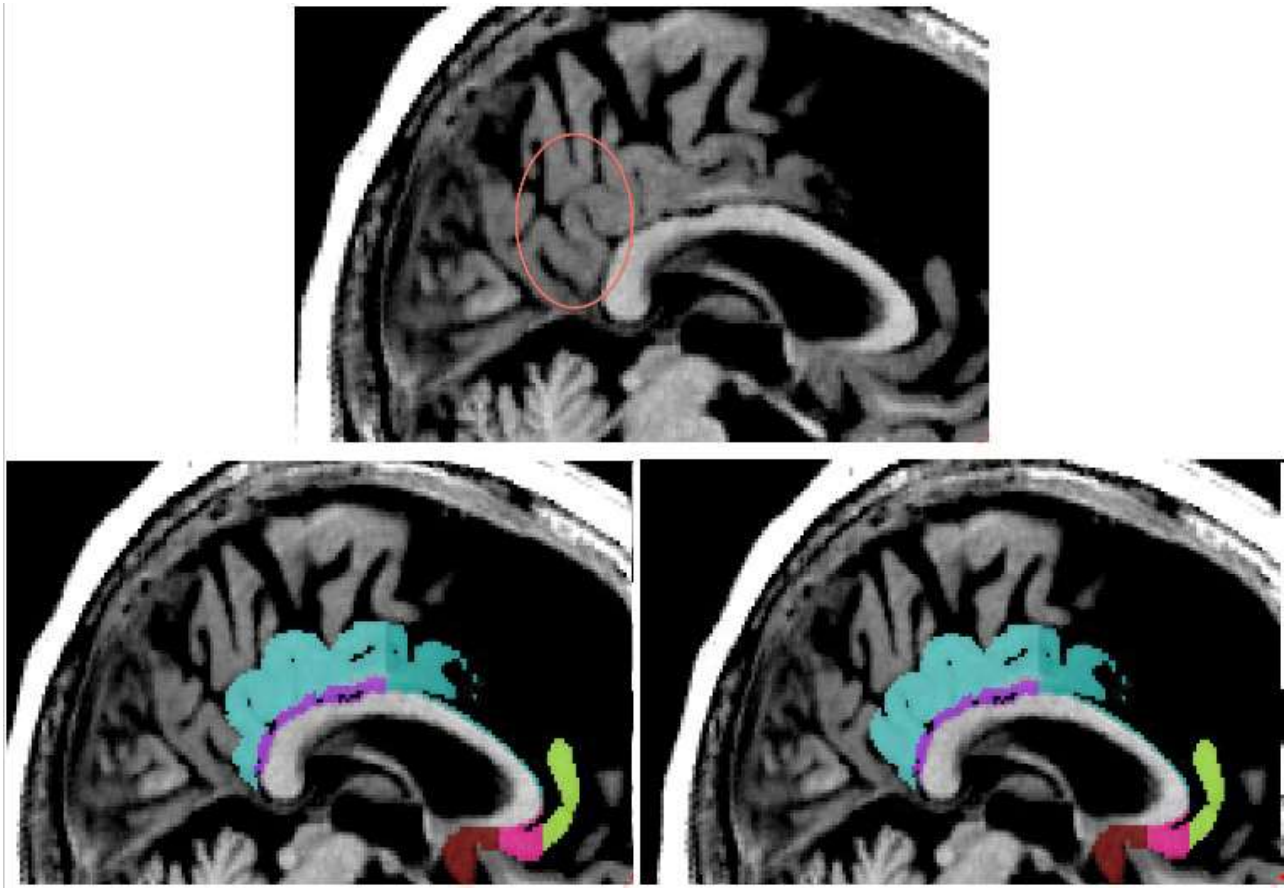

Figure 17: The picture above shows the spls inside the red circle. Note that it slightly resembles an "H" and also finishes before the cc end. Both pictures below show the segmented PCC, the left one is wrong and the right one is correct, since the PCC respects the cc orientation. Taken from our sample.

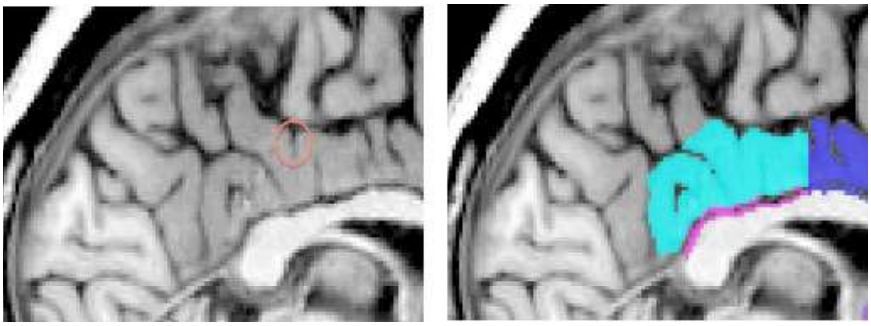

Figure 18: The fourth pattern of the mr and PCC relationship. The parcellation follows the "H" horizontal part, as shown in the right picture. Note a small vertical branch pointed by the red circle. It is not the branch to be connected with the spls because it is not parallel with the cas. Taken from our sample.

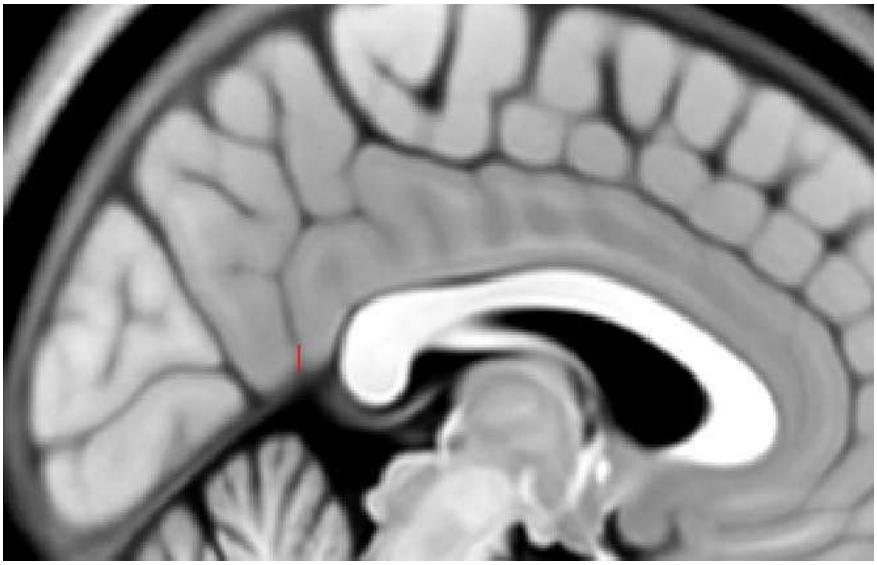

Figure 19: The straight down line connecting the spls end with the hemisphere end. Taken from an atlas by Fonov et al. (2009).

Go caudally through the coronal slices until there is not possible to see the splenium of the cc anymore. Then switch to the axial slices and set the ventral caudal border of PCC. That will be the most ventral axial slice on which the curvature of the splenium of the cc is visible, i.e., the axial slice right before the slice where the cc two sides are no longer connected through the splenium (Fig 8) (Jones et. al. 2006). That border makes you lose some parts of the Brodmann's area 23b and some RSC, but ensures you don't pick any parahippocampal cortex.

The RSC is the cortex ventral to the cas dorsal bank edge in the coronal view and rostral to the cas caudal bank edge in the axial slices (Fig 16).

Step 7: The Caudomedial Region (CMR).

The CMR is an intersection between PCC, RSC and parahippocampal cortices (Vogt et. al. 2001). It is parcellated mostly in sagittal slices, with corrections in axial slices when proper. Initially, take the most lateral sagittal slice in which it is still possible to see CSF inside the whole extension of the acals, i. e., the sulcus is not interrupted from its beginning in the calcarine and parieto-occipital sulci junction (Fig 20). The majority of our sample shows the acals interruption in its most rostral part, but sometimes it is interrupted more caudally.

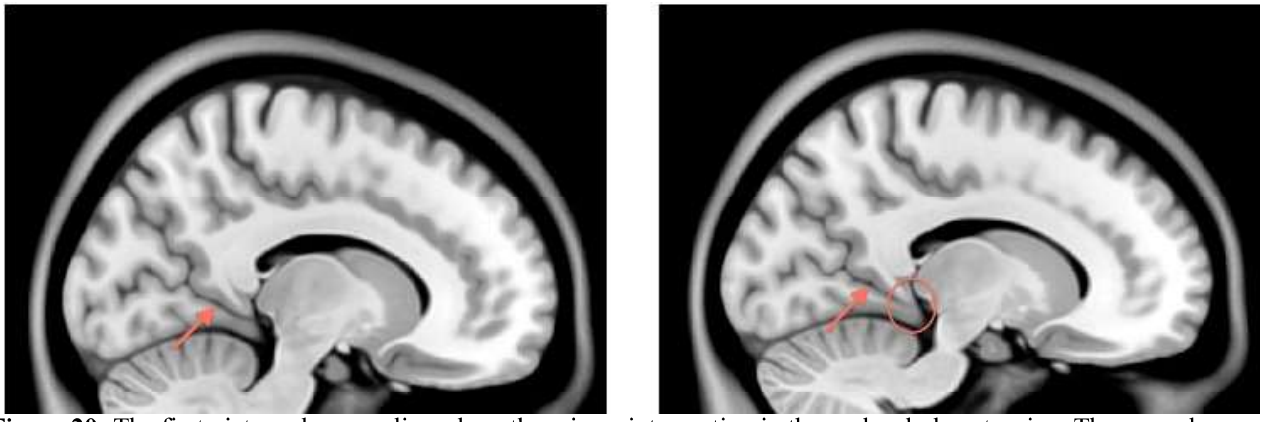

Figure 20: The first picture shows a slice where there is no interruption in the acals whole extension. The second one shows a more lateral view, in which it is not possible to see CSF throughout the entire acals. Red arrow = acals; red circle = the point where the acals interrupts. Taken from an atlas by Fonov et al. (2009).

The CMR segmentation follows a latero-medial orientation through sagittal slices. Its ventro-caudal limit is given by the acals, and, as the parcellation proceeds dorsally, by the same caudal limit set for the PCC end. The dorsal limit is the the first axial slice where the cc two sides are no longer connected through the splenium, i.e., the end of PCC + RSC (Fig 8). Finally, the rostral limit is the small stripe of CSF behind the thalamic pulvinar nucleus. Figure 21 is an example of a segmented CMR.

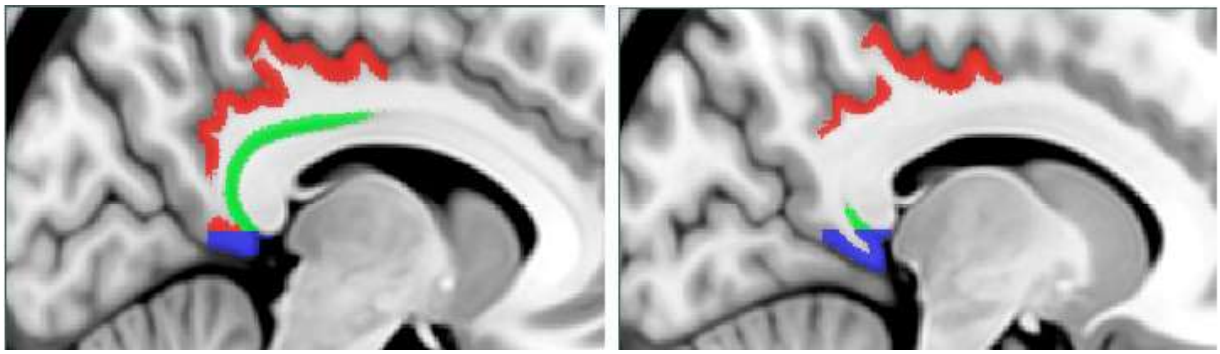

Figure 21: The CMR is shown in blue. The first picture is a more medial view of the same brain atlas. Note that the CMR caudal and dorsal limits stay unchanged in the right picture, still respecting the PCC caudal limit and the PCC + RSC ventral limit. Red = PCC; Green = RSC. Taken from an atlas by Fonov et al. (2009).

Step 8: The Subgenual Cortex (SGC).

The SGC starts in the most rostral coronal slice where the putamen appears (plane B). Go segmenting as you were continuing the cingulate segmentation (i. e. between the cingulate and callosal sulci). The cgs (or srs – see Step 5, “Variability specific rules”) will gradually disappear, while the ascs gradually forms itself as the cgs continuation. The SGC rostral boundaries are the ascs and the plane B slice, the latter in its dorsal part. The caudal boundary is the pscs, the dorsal is the rostrum of cc and the ventral is given by the merging of anterior and posterior subcallosal sulci, separating the SGC from the gyrus rectus. Go segmenting in a rostro-caudal direction on the coronal slices always correcting yourself by the medial sagittal ones, as you can see better the anatomic landmarks in the latter, but the cortex depth in the first. Figure 22 shows an example of a parcellated SGC.

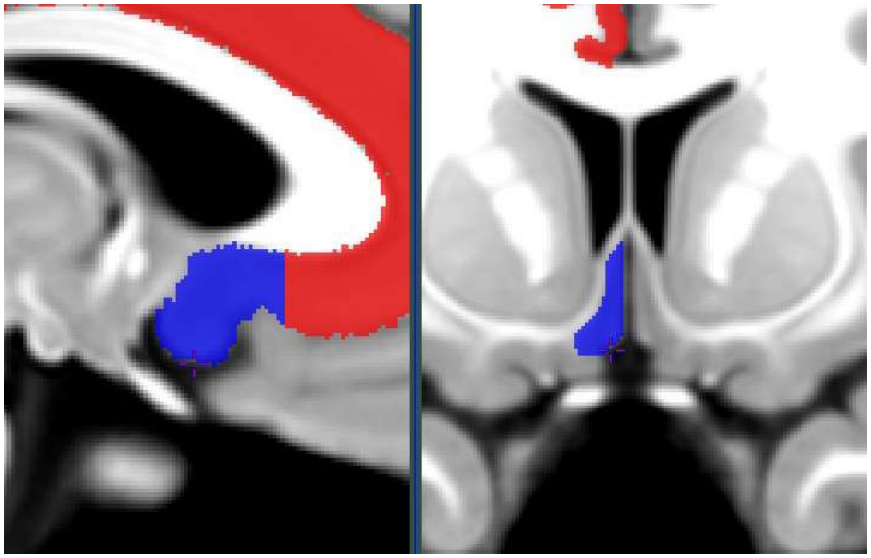

Figure 22: The SGC is shown in blue. The first picture is a sagittal slice and the second is a coronal one. Red = undivided cingulate cortex. Taken from an atlas by Fonov et al. (2009).

Variability specific rules:

In several individuals the cgs (or srs) does not connect with the ascs. When it happens, a line must be traced on the sagittal slices marking the shortest path uniting the cgs (srs) end with the ascs beginning.

Sometimes, the merging of both sulci is blurred. In order to separate the SGC from gyrus rectus in this case, trace a line connecting them in several sagittal slices, respecting their orientation.

When the ascs is not present (see Step 1), the SGC rostral landmark will be a straight line on sagittal slices from the rostrum of corpus callosum to the inferior margin of the frontal lobe.

REFERENCES

Bonilha L, Kobayashi E, Cendes F, Min Li L. 2004. Protocol for volumetric segmentation of medial temporal structures using high-resolution 3-D magnetic resonance imaging. Hum Brain Mapp. Jun;22(2):145-54.

Braak H. 1976. A primitive gigantopyramidal field buried in the depth of the cingulate sulcus of the human brain. Brain Res. Jun 11;109(2):219-23.

Crespo-Facorro B, Kim JJ, Andreasen NC, O'Leary DS, Wiser AK, Bailey JM, Harris G, Magnotta VA, 1999. Human frontal cortex: an MRI-based parcellation method. NeuroImage 10 (5), 500 – 519.

Fonov VS, Evans AC, McKinstry RC, Almli CR and Collins DL. 2009. Unbiased nonlinear average age-appropriate brain templates from birth to adulthood. Neuroimage. Jul; 47, Suppl 1:S102. Organization for Human Brain Mapping 2009 Annual Meeting.

Gunning FM, Cheng J, Murphy CF, Kanellopoulos D, Acuna J, Hoptman MJ, Klimstra S, Morimoto S, Weinberg J, Alexopoulos GS. 2009. Anterior cingulate cortical volumes and treatment remission of geriatric depression. Int J Geriatr Psychiatry. Aug;24(8):829-36.

Ichikawa N, Siegle GJ, Jones NP, Kamishima K, Thompson WK, Gross JJ, Ohira H. 2011. Feeling bad about screwing up: emotion regulation and action monitoring in the anterior cingulate cortex. Cogn Affect Behav Neurosci. Sep;11(3):354-71.

Jones BF, Barnes J, Uylings HB, Fox NC, Frost C, Witter MP, Scheltens P. 2006. Differential regional atrophy of the cingulate gyrus in Alzheimer disease: a volumetric MRI study. Cereb Cortex. Dec;16(12):1701-8.

Lindberg O, Ostberg P, Zandbelt BB, Oberg J, Zhang Y, Andersen C, Looi JC, Bogdanović N, Wahlund LO. 2009. Cortical morphometric subclassification of frontotemporal lobar degeneration. AJNR Am J Neuroradiol. Jun;30(6):1233-9.

McCormick LM, Ziebell S, Nopoulos P, Cassell M, Andreasen NC, Brumm M. 2006. Anterior cingulate cortex: an MRI-based parcellation method. Neuroimage. Sep;32(3):1167-75.

Ono M, Kubick S, Abernathey CD. 1990. Atlas of the Cerebral Sulci. Thieme, New York.

Paus T, Tomaiuolo F, Otaky N, MacDonald D, Petrides M, Atlas J, Morris R, Evans AC. 1996. Human cingulate and paracingulate sulci: pattern, variability, asymmetry, and probabilistic map. Cereb Cortex. Mar-Apr;6(2):207-14.

Richardson ME, Crocetti D, Clauss JA, Kraut MA, Mostofsky SH, Kaufmann WE. 2009. Manual MRI parcellation of the frontal lobe. Psychiatry Res. May 15; 172(2): 147–154.

Spasojević GD, Malobabić S, Suščević D, Stijak L, Nikolić V, Gojković I. 2011. Morphological variability of the subcallosal area of man. Surg Radiol Anat. May;33(4):313-8.

Vogt BA, Hof PR, Vogt LJ. 2004. Cingulate gyrus. In: Paxinos G, Mai JK, editors. The human nervous system. San Diego, CA: Academic Press. P 915—949.

Vogt BA, Vogt LJ, Perl DP, Hof PR. 2001. Cytology of human caudomedial cingulate, retrosplenial, and caudal parahippocampal cortices. J Comp Neurol. Sep 24;438(3):353-76.

PSYCHIATRY RESEARCH: NEUROIMAGING

The Official Publication of the International Society for Neuroimaging in Psychiatry

AUTHOR INFORMATION PACK

TABLE OF CONTENTS

ISSN: 0925-4927

DESCRIPTION

The *Neuroimaging* section of *Psychiatry Research* publishes manuscripts on positron emission tomography, magnetic resonance imaging, computerized electroencephalographic topography, regional cerebral blood flow, computed tomography, magnetoencephalography, autoradiography, post-mortem regional analyses, and other **imaging techniques**. Reports concerning results in **psychiatric disorders**, **dementias**, and the effects of **behaviorial tasks** and **pharmacological treatments** are featured. We also invite manuscripts on the methods of obtaining images and computer processing of the images themselves. Selected case reports are also published.

Benefits to authors
We also provide many author benefits, such as free PDFs, a liberal copyright policy, special discounts on Elsevier publications and much more. Please click here for more information on our author services.

Please see our Guide for Authors for information on article submission. If you require any further information or help, please visit our support pages: http://support.elsevier.com

AUDIENCE

Psychiatrists, Neurologists, Psychopharmacologists and Clinical Neurophysiologists.

IMPACT FACTOR

2013: 2.831 © Thomson Reuters Journal Citation Reports 2014

ABSTRACTING AND INDEXING

BIOSIS
Chemical Abstracts
Current Contents/Life Sciences
MEDLINE®
EMBASE
PsycINFO Psychological Abstracts
SIIC Data Bases
Scopus

EDITORIAL BOARD

GUIDE FOR AUTHORS

The Neuroimaging section of *Psychiatry Research*publishes manuscripts on positron emission tomography, magnetic resonance imaging, magnetic resonance spectroscopy, functional magnetic resonance imaging, single photon emission computed tumography, computerized electroencephalographic topography, regional cerebral blood flow, computed tomography, magnetoencephalography, autoradiography, post-mortem regional analyses, and other imaging techniques. Reports concerning results in psychiatric disorders, dementias and the effects of behavioral tasks and pharmacological treatments are featured. We also invite manuscripts on the methods of obtaining images and computer processing of the images themselves.

Preparation of manuscripts

Title page. The Title page should include the author byline, with names of authors on the same line(s). Superscript letters (a, b, c), not numerals, should be used to key institutional affiliation (if all authors are in the same department, the superscript letter should be omitted); an asterisk should be entered to designate the corresponding author. Underneath the byline, institutional affiliations should be listed (department, institution, city, state or province (if applicable) and country. Funding information should not be included on the title page but should instead be given following the Discussion section.In an asterisked Corresponding Author footnote at the bottom of the title page, telephone/fax numbers and e-mail address of the corresponding author should be provided; e-mail addresses, if desired, may also be provided for the co-authors (or co-corresponding author, if applicable).

Abstract. The Abstract should be 150-200 words for full-length articles and 75 words for brief reports, summarizing the aims of the study, the methods used, the results and the major conclusions. Do not include a summary at the end of the article. Note that *Psychiatry Research: Neuroimaging* does not use the structured abstract style; do not include bold-faced headings within the abstract. The Abstract should be a single paragraph. Do not include detailed statistics or p-values in the abstract; simply say "significant "or "non-significant."The Abstract should be followed by up to seven Key Words, which accord with the indexing

The abstract should be followed by up to seven key words should be listed which accord with the indexing conventions of Index Medicus. Note that the keywords should not duplicate words used in the title of the article, which will be automatically indexed.

Text. Although exceptions will be considered, manuscripts should not exceed 5000 words, and shorter manuscripts (e.g., 3000 words) are preferred. Each article should contain the following major headings: Introduction (preceded by arabic number 1.), Methods (preceded by number 2.), Results (preceded by number 3.), Discussion (preceded by number 4.), Acknowledgment (optional section following the discussion, which should not be preceded by a numeral), and References (should not be preceded by a numeral).

Subheadings should follow the numbering system used in the major heading; for example, the subheading "Subjects" within the Methods section should be flush left on a separate line and designated 2.1., the subheading "Procedures" should be designated 2.2., etc.

Lower level headings, if required, should also be numbered (e.g., "2.1.1. Patients." as a lower order heading under "2.1. Subjects."). Only the first letter of the first word of each heading should be capitalized.

The use of abbreviations within the text should be minimized, and each abbreviation, when introduced, must be defined and used onsistently thereafter. Systeme International measurements should be used. For products or instruments (do not abbreviate) used in the research reported, provide the name, city and country of the supplier in parentheses. All tables and figures must be referred to in the text.

Manuscript categories

Articles. Although exceptions will be considered, manuscripts should not exceed 5000 words, and shorter manuscripts (e.g., 3000 words) are preferred. Each article should contain the following major headings: Introduction (preceded by arabic number 1.), Methods (preceded by number 2.), Results (preceded by number 3.), Discussion (preceded by number 4.), Acknowledgment (optional section

following the discussion, which should not be preceded by a numeral), and References (should not be preceded by a numeral). Subheadings should follow the numbering system used in the major heading; for example, the subheading "Subjects" within the Methods section should be flush left on a separate line and designated 2.1., the subheading "Procedures" should be designated 2.2., etc. Lower level headings, if required, should also be numbered (e.g., "2.1.1. Patients." as a lower order heading under "2.1.Subjects."). Only the first letter of the first word of each heading should be capitalized.

Brief reports. Brief reports should not exceed 1500 words, including a 75-word abstract, 3 keywords, text, and references plus 1 table or 1 figure.

Case reports. Case reports will only be considered as Letters to the Editor (see following instructions).

Letters to the Editor. Letters to the Editor should be 750-1000 words or less. The Letter should not include a title page, abstract or key words. Authors' names and affiliations should be listed at the end of the Letter, along with the corresponding author's email address. There should be no more than 5 references, and no tables or figures.

Introduction. The introduction should be brief and explain the purpose of the study; an extensive review of the literature should be avoided, but directly relevant articles by other investigators, as well as by the authors themselves, must be cited. If the manuscript includes subjects who have been included in previous reports, references should be provided and the number of subjects whose data have been included elsewhere should be specified.

Methods. The Methods should contain sufficient detail to enable others to repeat the procedures without studying the references directly.

Results. The Results should summarize the most important data, and statistical correlations should be included. Tabular data should not be duplicated in the text; important points and trends should be pointed out. The final sentence should emphasize the importance attached to the observations.

Discussion. The discussion should relate directly to the study being reported and give perspective to the adequacy of the materials and methods for the purpose of the study. Results should be interpreted to lend meaning to the observations. Any discrepancies with previously published results should be explained. The paper should conclude with a brief statement regarding the significance of the study.

Acknowledgement. The Acknowledgement section is an optional section and should also be used for grant-support information.

Contributors. The individual contributions of each author should be briefly summarized.

Conflict of interest. All authors are requested to disclose any actual or potential conflict of interest including any financial, personal or other relationships with other people or organizations within three (3) years of beginning the work submitted that could inappropriately influence, or be perceived to influence, their work. Examples of potential conflicts of interest that should be disclosed include employment, consultancies, stock ownership (except for personal investment purposes equal to the lesser of one percent (1%) or USD 5000), honoraria, paid expert testimony, patent applications, registrations, and grants. If there are no conflicts of interest, authors should state that there are none.

Abbreviations. Define abbreviations at their first occurrence in the article. Abbreviations should be defined when they first occur in the abstract, in the text, and also in tables and figure legends. Once an abbreviation has been introduced in the main body of the text, it should be used throughout.

Statistical reporting. Statistical reporting should be complete, including at a minimum name of statistical test, test value, degrees of freedom where appropriate, and *p*-value. Italic font should be used for *n* (sample size) and statistical terms, e.g., *t, r, F, U, p*.

Submission of manuscripts

Once a manuscript has successfully been submitted via the online submission system, authors may track the status of their manuscript using the online submission system (details will be provided by e-mail). If your manuscript is accepted by the journal, subsequent tracking facilities are available on Elsevier's Author Gateway, using the unique reference number provided by Elsevier and corresponding author name (details will be provided by e-mail).

Authors may send queries concerning the submission process or journal procedures to the Managing Editor (E-mail: sherry.buchsbaum@gmail.com).

BEFORE YOU BEGIN

Ethics in publishing

For information on Ethics in publishing and Ethical guidelines for journal publication see http://www.elsevier.com/publishingethics and http://www.elsevier.com/journal-authors/ethics.

Human and animal rights

If the work involves the use of animal or human subjects, the author should ensure that the work described has been carried out in accordance with The Code of Ethics of the World Medical Association (Declaration of Helsinki) for experiments involving humans http://www.wma.net/en/30publications/10policies/b3/index.html; EU Directive 2010/63/EU for animal experiments http://ec.europa.eu/environment/chemicals/lab_animals/legislation_en.htm; Uniform Requirements for manuscripts submitted to Biomedical journals http://www.icmje.org. Authors should include a statement in the manuscript that informed consent was obtained for experimentation with human subjects. The privacy rights of human subjects must always be observed.

Conflict of interest

All authors must disclose any financial and personal relationships with other people or organizations that could inappropriately influence (bias) their work. Examples of potential conflicts of interest include employment, consultancies, stock ownership, honoraria, paid expert testimony, patent applications/ registrations, and grants or other funding. See also http://www.elsevier.com/conflictsofinterest. Further information and an example of a Conflict of Interest form can be found at: http://help.elsevier.com/app/answers/detail/a_id/286/p/7923.

Submission declaration

Submission of an article implies that the work described has not been published previously (except in the form of an abstract or as part of a published lecture or academic thesis or as an electronic preprint, see http://www.elsevier.com/postingpolicy), that it is not under consideration for publication elsewhere, that its publication is approved by all authors and tacitly or explicitly by the responsible authorities where the work was carried out, and that, if accepted, it will not be published elsewhere including electronically in the same form, in English or in any other language, without the written consent of the copyright-holder.

Changes to authorship

This policy concerns the addition, deletion, or rearrangement of author names in the authorship of accepted manuscripts:

Before the accepted manuscript is published in an online issue: Requests to add or remove an author, or to rearrange the author names, must be sent to the Journal Manager from the corresponding author of the accepted manuscript and must include: (a) the reason the name should be added or removed, or the author names rearranged and (b) written confirmation (e-mail, fax, letter) from all authors that they agree with the addition, removal or rearrangement. In the case of addition or removal of authors, this includes confirmation from the author being added or removed. Requests that are not sent by the corresponding author will be forwarded by the Journal Manager to the corresponding author, who must follow the procedure as described above. Note that: (1) Journal Managers will inform the Journal Editors of any such requests and (2) publication of the accepted manuscript in an online issue is suspended until authorship has been agreed.

After the accepted manuscript is published in an online issue: Any requests to add, delete, or rearrange author names in an article published in an online issue will follow the same policies as noted above and result in a corrigendum.

Copyright

This journal offers authors a choice in publishing their research: Open access and Subscription.

For subscription articles
Upon acceptance of an article, authors will be asked to complete a 'Journal Publishing Agreement' (for more information on this and copyright, see http://www.elsevier.com/copyright). An e-mail will be sent to the corresponding author confirming receipt of the manuscript together with a 'Journal Publishing Agreement' form or a link to the online version of this agreement.
Subscribers may reproduce tables of contents or prepare lists of articles including abstracts for internal circulation within their institutions. Permission of the Publisher is required for resale or distribution outside the institution and for all other derivative works, including compilations and translations (please consult http://www.elsevier.com/permissions). If excerpts from other copyrighted works are included, the author(s) must obtain written permission from the copyright owners and credit the source(s) in the article. Elsevier has preprinted forms for use by authors in these cases: please consult http://www.elsevier.com/permissions.

For open access articles
Upon acceptance of an article, authors will be asked to complete an 'Exclusive License Agreement' (for more information see http://www.elsevier.com/OAauthoragreement). Permitted reuse of open access articles is determined by the author's choice of user license (see http://www.elsevier.com/openaccesslicenses).

Retained author rights
As an author you (or your employer or institution) retain certain rights. For more information on author rights for:
Subscription articles please see http://www.elsevier.com/journal-authors/author-rights-and-responsibilities.
Open access articles please see http://www.elsevier.com/OAauthoragreement.

Role of the funding source
You are requested to identify who provided financial support for the conduct of the research and/or preparation of the article and to briefly describe the role of the sponsor(s), if any, in study design; in the collection, analysis and interpretation of data; in the writing of the report; and in the decision to submit the article for publication. If the funding source(s) had no such involvement then this should be stated.

Funding body agreements and policies
Elsevier has established agreements and developed policies to allow authors whose articles appear in journals published by Elsevier, to comply with potential manuscript archiving requirements as specified as conditions of their grant awards. To learn more about existing agreements and policies please visit http://www.elsevier.com/fundingbodies.

Open access
This journal offers authors a choice in publishing their research:

Open access
• Articles are freely available to both subscribers and the wider public with permitted reuse
• A open access publication fee is payable by authors or their research funder
Subscription
• Articles are made available to subscribers as well as developing countries and patient groups through our access programs (http://www.elsevier.com/access)
• No open access publication fee

All articles published open access will be immediately and permanently free for everyone to read and download. Permitted reuse is defined by your choice of one of the following Creative Commons user licenses:
Creative Commons Attribution-NonCommercial-ShareAlike (CC BY-NC-SA): for non-commercial purposes, lets others distribute and copy the article, to create extracts, abstracts and other revised versions, adaptations or derivative works of or from an article (such as a translation), to include in a collective work (such as an anthology), to text and data mine the article, as long as they credit the author(s), do not represent the author as endorsing their adaptation of the article, do not modify the article in such a way as to damage the author's honor or reputation, and license their new adaptations or creations under identical terms (CC BY-NC-SA).

Creative Commons Attribution-NonCommercial-NoDerivs (CC BY-NC-ND): for non-commercial purposes, lets others distribute and copy the article, and to include in a collective work (such as an anthology), as long as they credit the author(s) and provided they do not alter or modify the article.

Elsevier has established agreements with funding bodies, http://www.elsevier.com/fundingbodies. This ensures authors can comply with funding body open access requirements, including specific user licenses, such as CC BY. Some authors may also be reimbursed for associated publication fees. If you need to comply with your funding body policy, you can apply for the CC BY license after your manuscript is accepted for publication.

To provide open access, this journal has a publication fee which needs to be met by the authors or their research funders for each article published open access.
Your publication choice will have no effect on the peer review process or acceptance of submitted articles.

The publication fee for this journal is **3000**, excluding taxes. Learn more about Elsevier's pricing policy: http://www.elsevier.com/openaccesspricing.

Language (usage and editing services)

Please write your text in good English (American or British usage is accepted, but not a mixture of these). Authors who feel their English language manuscript may require editing to eliminate possible grammatical or spelling errors and to conform to correct scientific English may wish to use the English Language Editing service available from Elsevier's WebShop (http://webshop.elsevier.com/languageediting/) or visit our customer support site (http://support.elsevier.com) for more information.

Submission

Submission to this journal proceeds totally online and you will be guided stepwise through the creation and uploading of your files. The system automatically converts source files to a single PDF file of the article, which is used in the peer-review process. Please note that even though manuscript source files are converted to PDF files at submission for the review process, these source files are needed for further processing after acceptance. All correspondence, including notification of the Editor's decision and requests for revision, takes place by e-mail removing the need for a paper trail.

Submit your article
Please submit your article via http://ees.elsevier.com/psyn.

Referees

Please submit the names and institutional e-mail addresses of several potential referees. For more details, visit our Support site. Note that the editor retains the sole right to decide whether or not the suggested reviewers are used.

Editorial Policy
Submitted manuscripts will be reviewed anonymously by at least two referees. Should a revised manuscript be required by the editors, the authors are requested to resubmit their revised manuscript to the journal within 6 months time. Studies on humans submitted to the journal must comply with the principles laid down in the Declaration of Helsinki (Br Med J 1964; 2: 177-178). The editors retain the right to reject papers on the grounds that, in their opinion, the ethical justification is questionable. Manuscripts may be edited to improve clarity and expression.

Manuscripts that are not published and that are not resubmitted in revised form will be destroyed within 1 year of the date of submission.

PREPARATION

Use of word processing software

It is important that the file be saved in the native format of the word processor used. The text should be in single-column format. Keep the layout of the text as simple as possible. Most formatting codes will be removed and replaced on processing the article. In particular, do not use the word processor's options to justify text or to hyphenate words. However, do use bold face, italics, subscripts, superscripts etc. When preparing tables, if you are using a table grid, use only one grid for each individual table and not a grid for each row. If no grid is used, use tabs, not spaces, to align columns. The electronic text should be prepared in a way very similar to that of conventional manuscripts

(see also the Guide to Publishing with Elsevier: http://www.elsevier.com/guidepublication). Note that source files of figures, tables and text graphics will be required whether or not you embed your figures in the text. See also the section on Electronic artwork.
To avoid unnecessary errors you are strongly advised to use the 'spell-check' and 'grammar-check' functions of your word processor.

Article structure

The Abstract should be 150-200 words for full-length articles and 75 words for brief reports.

Subdivision - numbered sections
Divide your article into clearly defined and numbered sections. Subsections should be numbered 1.1 (then 1.1.1, 1.1.2, ...), 1.2, etc. (the abstract is not included in section numbering). Use this numbering also for internal cross-referencing: do not just refer to 'the text'. Any subsection may be given a brief heading. Each heading should appear on its own separate line.

Essential title page information

• ***Title.*** Concise and informative. Titles are often used in information-retrieval systems. Avoid abbreviations and formulae where possible.
• ***Author names and affiliations.*** Where the family name may be ambiguous (e.g., a double name), please indicate this clearly. Present the authors' affiliation addresses (where the actual work was done) below the names. Indicate all affiliations with a lower-case superscript letter immediately after the author's name and in front of the appropriate address. Provide the full postal address of each affiliation, including the country name and, if available, the e-mail address of each author.
• ***Corresponding author.*** Clearly indicate who will handle correspondence at all stages of refereeing and publication, also post-publication. **Ensure that phone numbers (with country and area code) are provided in addition to the e-mail address and the complete postal address. Contact details must be kept up to date by the corresponding author.**
• ***Present/permanent address.*** If an author has moved since the work described in the article was done, or was visiting at the time, a 'Present address' (or 'Permanent address') may be indicated as a footnote to that author's name. The address at which the author actually did the work must be retained as the main, affiliation address. Superscript Arabic numerals are used for such footnotes.

Abstract

A concise and factual abstract is required. The abstract should state briefly the purpose of the research, the principal results and major conclusions. An abstract is often presented separately from the article, so it must be able to stand alone. For this reason, References should be avoided, but if essential, then cite the author(s) and year(s). Also, non-standard or uncommon abbreviations should be avoided, but if essential they must be defined at their first mention in the abstract itself.

Graphical abstract

A Graphical abstract is optional and should summarize the contents of the article in a concise, pictorial form designed to capture the attention of a wide readership online. Authors must provide images that clearly represent the work described in the article. Graphical abstracts should be submitted as a separate file in the online submission system. Image size: Please provide an image with a minimum of 531 × 1328 pixels (h × w) or proportionally more. The image should be readable at a size of 5 × 13 cm using a regular screen resolution of 96 dpi. Preferred file types: TIFF, EPS, PDF or MS Office files. See http://www.elsevier.com/graphicalabstracts for examples.
Authors can make use of Elsevier's Illustration and Enhancement service to ensure the best presentation of their images also in accordance with all technical requirements: Illustration Service.

Highlights

Highlights are mandatory for this journal. They consist of a short collection of bullet points that convey the core findings of the article and should be submitted in a separate file in the online submission system. Please use 'Highlights' in the file name and include 3 to 5 bullet points (maximum 85 characters, including spaces, per bullet point). See http://www.elsevier.com/highlights for examples.

Keywords

Immediately after the abstract, provide a maximum of 6 keywords, using American spelling and avoiding general and plural terms and multiple concepts (avoid, for example, 'and', 'of'). Be sparing with abbreviations: only abbreviations firmly established in the field may be eligible. These keywords will be used for indexing purposes.

Abbreviations

Define abbreviations that are not standard in this field in a footnote to be placed on the first page of the article. Such abbreviations that are unavoidable in the abstract must be defined at their first mention there, as well as in the footnote. Ensure consistency of abbreviations throughout the article.

In the abstract, define all abbreviations so that electronic searches for commonly used abbreviations or the full name can be successful. Avoid abbreviations unique to the current article so as to widen the circle of readers. We recognize that many abbreviations or acronyms may be more familiar to the reader than the full name. However abbreviations and acronyms used by relatively few other published reports or abbreviations with several alternatate meanings in data base searches should always be spelled out throughout the report.

Acknowledgements

Collate acknowledgements in a separate section at the end of the article before the references and do not, therefore, include them on the title page, as a footnote to the title or otherwise. List here those individuals who provided help during the research (e.g., providing language help, writing assistance or proof reading the article, etc.).

Footnotes

Footnotes should be used sparingly. Number them consecutively throughout the article, using superscript Arabic numbers. Many wordprocessors build footnotes into the text, and this feature may be used. Should this not be the case, indicate the position of footnotes in the text and present the footnotes themselves separately at the end of the article. Do not include footnotes in the Reference list.

Table footnotes

Indicate each footnote in a table with a superscript lowercase letter.

Artwork

Electronic artwork

General points

• Make sure you use uniform lettering and sizing of your original artwork.
• Embed the used fonts if the application provides that option.
• Aim to use the following fonts in your illustrations: Arial, Courier, Times New Roman, Symbol, or use fonts that look similar.
• Number the illustrations according to their sequence in the text.
• Use a logical naming convention for your artwork files.
• Provide captions to illustrations separately.
• Size the illustrations close to the desired dimensions of the printed version.
• Submit each illustration as a separate file.

A detailed guide on electronic artwork is available on our website:
http://www.elsevier.com/artworkinstructions
You are urged to visit this site; some excerpts from the detailed information are given here.

Formats

If your electronic artwork is created in a Microsoft Office application (Word, PowerPoint, Excel) then please supply 'as is' in the native document format.
Regardless of the application used other than Microsoft Office, when your electronic artwork is finalized, please 'Save as' or convert the images to one of the following formats (note the resolution requirements for line drawings, halftones, and line/halftone combinations given below):
EPS (or PDF): Vector drawings, embed all used fonts.
TIFF (or JPEG): Color or grayscale photographs (halftones), keep to a minimum of 300 dpi.
TIFF (or JPEG): Bitmapped (pure black & white pixels) line drawings, keep to a minimum of 1000 dpi.
TIFF (or JPEG): Combinations bitmapped line/half-tone (color or grayscale), keep to a minimum of 500 dpi.

Please do not:

• Supply files that are optimized for screen use (e.g., GIF, BMP, PICT, WPG); these typically have a low number of pixels and limited set of colors;
• Supply files that are too low in resolution;
• Submit graphics that are disproportionately large for the content.

Color artwork
Please make sure that artwork files are in an acceptable format (TIFF (or JPEG), EPS (or PDF), or MS Office files) and with the correct resolution. If, together with your accepted article, you submit usable color figures then Elsevier will ensure, at no additional charge, that these figures will appear in color on the Web (e.g., ScienceDirect and other sites) regardless of whether or not these illustrations are reproduced in color in the printed version. **For color reproduction in print, you will receive information regarding the costs from Elsevier after receipt of your accepted article**. Please indicate your preference for color: in print or on the Web only. For further information on the preparation of electronic artwork, please see http://www.elsevier.com/artworkinstructions.
Please note: Because of technical complications which can arise by converting color figures to 'gray scale' (for the printed version should you not opt for color in print) please submit in addition usable black and white versions of all the color illustrations.

Illustration services

Elsevier's WebShop (http://webshop.elsevier.com/illustrationservices) offers Illustration Services to authors preparing to submit a manuscript but concerned about the quality of the images accompanying their article. Elsevier's expert illustrators can produce scientific, technical and medical-style images, as well as a full range of charts, tables and graphs. Image 'polishing' is also available, where our illustrators take your image(s) and improve them to a professional standard. Please visit the website to find out more.

Tables

Number tables consecutively in accordance with their appearance in the text. Place footnotes to tables below the table body and indicate them with superscript lowercase letters. Avoid vertical rules. Be sparing in the use of tables and ensure that the data presented in tables do not duplicate results described elsewhere in the article.

References

Citation in text
Please ensure that every reference cited in the text is also present in the reference list (and vice versa). Any references cited in the abstract must be given in full. Unpublished results and personal communications are not recommended in the reference list, but may be mentioned in the text. If these references are included in the reference list they should follow the standard reference style of the journal and should include a substitution of the publication date with either 'Unpublished results' or 'Personal communication'. Citation of a reference as 'in press' implies that the item has been accepted for publication.

Reference style
Literature citations. References in the text to literature cited should be given by the surname of the author(s), followed by the year of publication in parentheses, e.g., Smith and Smith (2011) or (Allen et al., 2006; Smith, 2008a, 2008; Jones and Jones, 2013). For three or more authors, the surname ofthe first author followed by et al. should be used. For citations to articles with two authors, use “and” instead of ampersand (Jones and Smith, 2010). References should be arranged in alphabetical order by first author and should not be numbered. For single-authored articles, if more than one article by the same author is included, list each reference in chronological order. If both articles were published in the same year, alphabetize by the first major word of the article title and designate the first listed article as "a," the second as "b," etc. For multi-authored articles, list in alphabetical order by (1) last name of first author, (2) last name of second author, etc. If the names of all authors are identical, list in chronological order. If both authors' names and year of publication are the same, alphabetize by the first major word of the article title.

Provide the last names and first initials of all authors (do not use et al. in the reference list). Journal titles should not be abbreviated; provide the journal's full name. Do not italicize journal or book titles. Be sure that all references are complete: Journal articles should include authors, year of publication, article title, full journal name, volume number, and beginning and concluding page numbers. Book chapters should include authors, year of publication, chapter title, name(s) of volume editor(s), volume title, volume number (if any), name of publisher, city of publication, and page numbers. Books should include author(s) or editor(s), year of publication, book title, publisher, and city of publication. Include only references that have been cited in the text. Provide the names of all authors; do not use “et al.” in the reference list.

Examples of typical types of references follow. In addition to the particular reference styles, the examples illustrate the order in which references should be listed and give examples of "a" and "b" designations.

Bernstein, T.M., 1985. The Careful Writer: A Modern Guide to English Usage. Atheneum, New York.
Buchsbaum, M.S., 1990. Frontal lobes, basal ganglia, temporal lobes--three sites for schizophrenia? Schizophrenia Bulletin 16, 377-378.
Buchsbaum, M.S., Holcomb, H.H., DeLisi, L.E., Hazlett, E., 1986. Brain imaging in affective disorders. In:Rush, A.J., Altshuler, K.Z. (Eds.), Depression: Basic Mechanisms, Diagnosis and Treatment. The Guilford Press, New York, pp. 126-142.
Issa, F., Gerhardt, G.A., Bartko, J.J., Suddath, R.L., Lynch, M. Gamache, P.H., Freedman, R., Wyatt, R.J., Kirch, D.G., 1994a. A multidimensional approach to analysis of cerebrospinal fluid biogenic amines in schizophrenia: I. Comparisons with healthy control subjects and neuroleptic-treated/ unmedicated pairs analyses. Psychiatry Research 52, 237-249.
Issa, F., Kirch, D.G., Gerhardt, G.A., Bartko, J.J., Suddath, R.L., Freedman, R., Wyatt, R.J., 1994b. A multidimensional approach to analysis of cerebrospinal fluid biogenic amines in schizophrenia: II. Correlations with psychopathology. Psychiatry Research 52, 251-258.
Strunk, W., White, E.B., 1979. The Elements of Style, 3rd ed. MacMillan, New York.

The correctness of the reference list is the entire responsibility of the author! Please check it carefully and remember to recheck when your article has been revised. Unpublished results should not be included in the reference list but, rather, should be quoted in the text (Smith and co-workers, unpublished results).

Reference links
Increased discoverability of research and high quality peer review are ensured by online links to the sources cited. In order to allow us to create links to abstracting and indexing services, such as Scopus, CrossRef and PubMed, please ensure that data provided in the references are correct. Please note that incorrect surnames, journal/book titles, publication year and pagination may prevent link creation. When copying references, please be careful as they may already contain errors. Use of the DOI is encouraged.

Web references
As a minimum, the full URL should be given and the date when the reference was last accessed. Any further information, if known (DOI, author names, dates, reference to a source publication, etc.), should also be given. Web references can be listed separately (e.g., after the reference list) under a different heading if desired, or can be included in the reference list.

Journal abbreviations source
Journal names should be abbreviated according to the List of Title Word Abbreviations: http://www.issn.org/services/online-services/access-to-the-ltwa/.

Video data

Elsevier accepts video material and animation sequences to support and enhance your scientific research. Authors who have video or animation files that they wish to submit with their article are strongly encouraged to include links to these within the body of the article. This can be done in the same way as a figure or table by referring to the video or animation content and noting in the body text where it should be placed. All submitted files should be properly labeled so that they directly relate to the video file's content. In order to ensure that your video or animation material is directly usable, please provide the files in one of our recommended file formats with a preferred maximum size of 50 MB. Video and animation files supplied will be published online in the electronic version of your article in Elsevier Web products, including ScienceDirect: http://www.sciencedirect.com. Please supply 'stills' with your files: you can choose any frame from the video or animation or make a separate image. These will be used instead of standard icons and will personalize the link to your video data. For more detailed instructions please visit our video instruction pages at http://www.elsevier.com/artworkinstructions. Note: since video and animation cannot be embedded in the print version of the journal, please provide text for both the electronic and the print version for the portions of the article that refer to this content.

AudioSlides

The journal encourages authors to create an AudioSlides presentation with their published article. AudioSlides are brief, webinar-style presentations that are shown next to the online article on ScienceDirect. This gives authors the opportunity to summarize their research in their own words and

to help readers understand what the paper is about. More information and examples are available at http://www.elsevier.com/audioslides. Authors of this journal will automatically receive an invitation e-mail to create an AudioSlides presentation after acceptance of their paper.

Supplementary data

Elsevier accepts electronic supplementary material to support and enhance your scientific research. Supplementary files offer the author additional possibilities to publish supporting applications, high-resolution images, background datasets, sound clips and more. Supplementary files supplied will be published online alongside the electronic version of your article in Elsevier Web products, including ScienceDirect: http://www.sciencedirect.com. In order to ensure that your submitted material is directly usable, please provide the data in one of our recommended file formats. Authors should submit the material in electronic format together with the article and supply a concise and descriptive caption for each file. For more detailed instructions please visit our artwork instruction pages at http://www.elsevier.com/artworkinstructions.

3D neuroimaging

You can enrich your online articles by providing 3D neuroimaging data in NIfTI format. This will be visualized for readers using the interactive viewer embedded within your article, and will enable them to: browse through available neuroimaging datasets; zoom, rotate and pan the 3D brain reconstruction; cut through the volume; change opacity and color mapping; switch between 3D and 2D projected views; and download the data. The viewer supports both single (.nii) and dual (.hdr and .img) NIfTI file formats. Recommended size of a single uncompressed dataset is 100 MB or less. Multiple datasets can be submitted. Each dataset will have to be zipped and uploaded to the online submission system via the '3D neuroimaging data' submission category. Please provide a short informative description for each dataset by filling in the 'Description' field when uploading a dataset. Note: all datasets will be available for downloading from the online article on ScienceDirect. If you have concerns about your data being downloadable, please provide a video instead. For more information see: http://www.elsevier.com/3DNeuroimaging.

Brain images and statistical images

Brain images should be of sufficient size that small marked regions are clearly visible. Large areas of surrounding black background should be minimized so that the brain images make up the majority of the illustration. Enlargements of portions of the brain should be considered as an additional part of the illustration.

In color illustrations please provide a color bar with scale points marked so that the colors will be interpretable.

The legend to the figure should mention the right-left orientation of the figure.

Submission checklist

The following list will be useful during the final checking of an article prior to sending it to the journal for review. Please consult this Guide for Authors for further details of any item.

Ensure that the following items are present:

One author has been designated as the corresponding author with contact details:

- E-mail address
- Full postal address
- Phone numbers

All necessary files have been uploaded, and contain:

- Keywords
- All figure captions
- All tables (including title, description, footnotes)

Further considerations

- Manuscript has been 'spell-checked' and 'grammar-checked'
- References are in the correct format for this journal
- All references mentioned in the Reference list are cited in the text, and vice versa
- Permission has been obtained for use of copyrighted material from other sources (including the Web)
- Color figures are clearly marked as being intended for color reproduction on the Web (free of charge) and in print, or to be reproduced in color on the Web (free of charge) and in black-and-white in print
- If only color on the Web is required, black-and-white versions of the figures are also supplied for printing purposes

For any further information please visit our customer support site at http://support.elsevier.com.

AFTER ACCEPTANCE

Use of the Digital Object Identifier

The Digital Object Identifier (DOI) may be used to cite and link to electronic documents. The DOI consists of a unique alpha-numeric character string which is assigned to a document by the publisher upon the initial electronic publication. The assigned DOI never changes. Therefore, it is an ideal medium for citing a document, particularly 'Articles in press' because they have not yet received their full bibliographic information. Example of a correctly given DOI (in URL format; here an article in the journal *Physics Letters B*):
http://dx.doi.org/10.1016/j.physletb.2010.09.059
When you use a DOI to create links to documents on the web, the DOIs are guaranteed never to change.

Online proof correction

Corresponding authors will receive an e-mail with a link to our online proofing system, allowing annotation and correction of proofs online. The environment is similar to MS Word: in addition to editing text, you can also comment on figures/tables and answer questions from the Copy Editor. Web-based proofing provides a faster and less error-prone process by allowing you to directly type your corrections, eliminating the potential introduction of errors.
If preferred, you can still choose to annotate and upload your edits on the PDF version. All instructions for proofing will be given in the e-mail we send to authors, including alternative methods to the online version and PDF.
We will do everything possible to get your article published quickly and accurately - please upload all of your corrections within 48 hours. It is important to ensure that all corrections are sent back to us in one communication. Please check carefully before replying, as inclusion of any subsequent corrections cannot be guaranteed. Proofreading is solely your responsibility. Note that Elsevier may proceed with the publication of your article if no response is received.

Offprints

The corresponding author, at no cost, will be provided with a personalized link providing 50 days free access to the final published version of the article on ScienceDirect. This link can also be used for sharing via email and social networks. For an extra charge, paper offprints can be ordered via the offprint order form which is sent once the article is accepted for publication. Both corresponding and co-authors may order offprints at any time via Elsevier's WebShop (http://webshop.elsevier.com/myarticleservices/offprints). Authors requiring printed copies of multiple articles may use Elsevier WebShop's 'Create Your Own Book' service to collate multiple articles within a single cover (http://webshop.elsevier.com/myarticleservices/booklets).

AUTHOR INQUIRIES

You can track your submitted article at http://help.elsevier.com/app/answers/detail/a_id/89/p/8045/. You can track your accepted article at http://www.elsevier.com/trackarticle. You are also welcome to contact Customer Support via http://support.elsevier.com.